

Universität Stuttgart

INSTITUT FÜR  
MECHANIK

# **The Influence of Joint Parameters on Dynamic Response of Structures**

**Master Thesis**

von

**Darong Jin**

durchgeführt am

**Institut für Angewandte und Experimentelle Mechanik**

**Universität Stuttgart**

**Institutsleiter: Prof. Dr.-Ing. habil. L. Gaul**

**Betreuer: Dipl.-Ing. Sergey Bograd**

**May 2011**

I hereby declare that I have written this work independently, yet not otherwise provided for audit purposes, other than those specified sources or equipment used as well as a letter or in a quotes such was characterized.

Stuttgart, May 23, 2011

Darong Jin

# Contents

<b>1. Introduction</b>	<b>1</b>
1.1. Introduction and Motivation . . . . .	1
1.2. Previous Work . . . . .	3
1.3. Objectives and Tasks . . . . .	4
<b>2. Theory</b>	<b>5</b>
2.1. Analytical Modal Analysis . . . . .	6
2.1.1. Spatial Model to Response Model . . . . .	7
2.1.2. Modal Model to Response Model . . . . .	10
2.2. Experimental Modal Analysis . . . . .	12
2.2.1. Experiment Process . . . . .	12
2.2.2. Modal Parameter Estimation Methods . . . . .	13
2.2.3. Universal File Format (UFF) . . . . .	19
2.3. FE Simulation . . . . .	19
<b>3. Design the System</b>	<b>23</b>
3.1. Criteria . . . . .	23
3.2. Design . . . . .	24
3.2.1. Assumption . . . . .	24
3.2.2. Sturcture . . . . .	24
3.2.3. Simulation . . . . .	24
<b>4. Analytical approach</b>	<b>31</b>
4.1. Analytical Data Sets Creation . . . . .	31
4.1.1. Analytical Data Sets With SISO Modal Model . . . . .	32
4.1.2. Analytical Data Sets With MIMO Modal Model . . . . .	33
4.1.3. Analytical Data Sets With MIMO Spatial Model . . . . .	33
4.2. Investigation of Modal Parameter Estimation Methods . . . . .	34
4.2.1. Pole Selecting Methods . . . . .	35
4.2.2. Frequency Resolution . . . . .	39

---

4.2.3. Modal Parameter Estimation Methods . . . . .	41
<b>5. Experiment and Simulation</b>	<b>45</b>
5.1. Experiment . . . . .	45
5.1.1. Experimental System Description . . . . .	45
5.1.2. Experimental Procedure . . . . .	49
5.1.3. Data Processing . . . . .	53
5.2. Simulation . . . . .	58
5.2.1. Adjust Material Properties . . . . .	58
5.2.2. Thin Layer Method . . . . .	60
<b>6. Conclusions and Recommendations</b>	<b>69</b>
6.1. Conclusions . . . . .	69
6.2. Recommendations . . . . .	70
<b>A. Appendix</b>	<b>73</b>
A.1. MATLAB codes . . . . .	73
A.2. ANSYS codes . . . . .	74
A.3. Blueprint . . . . .	77
<b>List of Figures</b>	<b>82</b>
<b>List of Tables</b>	<b>84</b>
<b>Bibliography</b>	<b>87</b>

# 1. Introduction

## 1.1. Introduction and Motivation

Nowadays, the daily life cannot separate apart from the mechanical systems and structures of mechanical systems are getting more and more complicated and sophisticated. As examples for structure with numerous joints are showed in figure 1.1. The structures tend to contain a giant numbers of joints in the system which are one of the most important factors that influence the dynamic response of the system. Investigation of the relationship between the joint characteristics and the dynamical properties of structure is important for a various fields of research and industry.



**Air bus 380**



**London Eye**



**BMW Z4 sDrive35is**



**Oscillating electric razor**

**Figure 1.1.:** Examples of mechanical systems for daily life with numerous joints

The vibrations and noises produced by mechanical systems serve as an important criterion for customers. During the traveling with automobiles or airplanes, the vibrations and the noises are big annoyance factors which make the journey tired and unpleasant. These are both affected by the dynamic properties of joint especially the damping property. Even though the eigenfrequencies and mode shapes can be predicted successfully by existing Finite Element Method (FEM) software. However, the damping property is still cannot be determined accurately with commercial FEM software since less attention has paid to this fields of study.

The damping property is related to the dissipated energy during the dynamic process. The dissipated energy is the culprit for vibrations and noises which are harmful for systems and cause the fracture of systems. It is critical to design and analysis the vibrating structures with respect to damping properties, since the dynamic response of structures and transmission of vibrations to the environment is closely depended on the damping mechanisms.

One of the existing approaches for dynamic analysis of mechanical systems is the Experimental Modal Analysis (EMA) which is an experimental method used to extract structural dynamic properties in terms of its modal parameters such as eigenfrequencies, damping ratio as well as mode shapes. The general steps of EMA are: first, acquire Frequency Response Functions (FRF) in the form of Universal File Format (UFF) from the impact hammer experiment or experiment with shaker; second, from these measured FRFs, Modal Parameter Estimation (MPE) with several different methods is carried out and the modal parameters can be obtained as results. There are numbers of MPE methods and the details about these methods are discussed in section 2.2.2. In the thesis, several analytical modal data sets are created to compare these methods with the software X-Modal II which is developed by the Structural Dynamics Research Laboratory of University of Cincinnati (UC-SDRL). The damping is very sensitive, as a consequence, the accuracy of these estimated modal parameters is greatly affected by the method applied along with the other factors mentioned in section 4.2.

In order to reduce product development periods and associated costs, nowadays, the industry is changing from the traditional ways of design to the Computer Aided Design (CAD), the Computer Aided Simulation and the Computer Aided Manufacturing (CAM). This means that the dynamical properties of a structure can be predicted by the computer simulations before the physical prototype is available. One of the standard approaches that allow the prediction of the vibration behavior for mechanical products is the Finite Element (FE) simulation. Figuring out the relations between the joint characteristic and the dynamic properties is the basic task and fundamentals for computer simulations. In last years, it has reached a significant improvement and ap-

plied successfully to the software to estimate the eigenfrequencies and mode shapes of complicated structures. However, the prediction of damping properties of structure, in other words, the dissipative properties still cannot be determined accurately[23].

Therefore, there is an urgent need to develop a strong reliable dynamic analysis tools which provide understandings of the interrelation between the joint characteristics and dynamic properties. The joint characteristics of the structure contain contact pressure and the distribution etc; the dynamic properties of the structure include eigenfrequencies and mode shapes as well as the damping properties.

## 1.2. Previous Work

To give a brief overview of the ongoing work, the previous works which have taken place in the mentioned research fields will be outlined here.

ANGEL MOISES IGLESIAS [10] did an investigation of four modal parameter estimation methods both in time domain and frequency domain with respect to the damping ratio. After introducing these modal parameter estimation methods, he compared the methods with Single Input Single Output (SISO) analytical data sets as well as the experiment data sets in the form of Frequency Response Functions (FRF) or Impulse Response Function (IRF). This work shows that the time domain methods result in better estimation with analytical data sets.

ALLEMANG, BROWN, PHILLIPS, ADAMS, MAIA and SILVA [21] [19] [20] [17] [1] [15] provide the fundamentals of analytical modal analysis and experimental modal analysis. They also give relatively detail descriptions of the existing modal parameter estimation methods. The advantages and disadvantages have been discussed. They also provide the introduction about the software X-Modal II which is developed by UC-SDRL which using different MPE methods to obtain the modal parameters.

Many works has been done in the research fields of joint modeling by BOGRAD, SCHMIT and GAUL [23] [22] [9]. They summarized the works have been done and provide the overview of joint modeling. Also from their works, the damping properties of system were considered as the combination of material damping and joint patch damping. They provide the experimental determination of two kinds of damping properties. Several different possibilities to implement the described models into the FEM have been investigated. One of these is to express the damping properties in terms of imaginary parts of the complex stiffness matrix. From the result of simulation and experiment with U-shaped structure made by thin plate with one of the implementation FEM (Thin layer methods), the existence of certain relations between joint characteristics and dynamic properties of the structure can be noticed.

### 1.3. Objectives and Tasks

The goal of the master thesis is to investigate the interrelation between different joint characteristics and the dynamic properties (modal parameters) of the assembled structure. The first task is to design simple structures of system which can provide different joint characteristics and fulfills certain criteria. The second problem is to investigate the modal parameter estimation methods with respect to several analytical data sets with low damping ratio. Then the investigation of the interrelation between different joint characteristics and the dynamic properties with the data sets acquired from impact hammer experiments is carried out. At last, the simulation with thin layer methods applied with the parameters given was performed to verify the investigation made by the previous chapters. The following outlines of the thesis are showed below.

In Chapter 2, the theories of the method and experiment were presented. For the analytical modal analysis, theories about modal model and spatial model are discussed; for experimental modal analysis, the procedure for the experiment, the modal parameter estimation methods and the brief knowledge of universal file format were summarized and introduced; for the Finite Element simulation, the detail theories about the simulation with the thin layer method and how it is related to ANSYS are provided.

In Chapter 3, the system with multiple joint characteristics was designed and manufactured. The procedure to check whether the structure satisfies the criteria was presented.

In Chapter 4, here we created several analytical data sets with the MATLAB code and used the data sets to investigate the modal parameter estimation methods with respect to several factors, including pole selecting method; frequency resolution and also different MPE methods applied.

In Chapter 5, here we talked the detail about the experiment and the simulation. In the first part, we gave the detail description, the procedure and the important points about the experiment, then the result was given, the data processing was operated and the brief conclusion was made.

In Chapter 6, Summarization of the important points over the entire master thesis was made, and then the recommendations for the further works were given.

In Appendix A the main part of MATLAB code to create the analytical model, the ANSYS code to perform the simulation with thin layer element method and the blueprints of the structures used in the thesis are given.



## 2. Theory

This chapter will show the detail theories which are related to the thesis, including analytical and experimental modal analysis, modal parameter estimation methods, and Finite Element simulation with thin layer elements method. For analytical modal analysis, the theories used to develop the analytical model data sets which will be used in comparison with different modal parameter estimation methods are discussed. For experimental modal analysis, the procedure applied to establish the experiment is introduced. For modal parameter estimation methods, the brief introduction and summarization of the theories of the MPE methods used in our data processing stage as well as the knowledge about universal file format was presented. At last, theories related to the simulation with thin layer method were discussed.

Assumptions [19] [20] for analytical modal analysis and experiment modal analysis was presented as following.

- The structure must be a linear system which means the system must be represented by a set of linear, second order differential equations.
- The structure must be time invariant during the dynamic process. This implies that the coefficients in the linear, second order differential equations are constants with respect to time.
- The structure must be observable. This means that the system characteristics describing the dynamic properties can be measured, in other words, there are sufficient sensors to adequately describe the input-output characteristics of the system. A linear system is observable if and only if the initial state can be determined from a finite interval of the output signals.
- The structure obeys Maxwell's reciprocity theorem. This implies the following: if one measures the frequency response function between points p and q by exciting at p and measuring the response at q, the same frequency response function will be measured by exciting at q and measuring the response at p which means  $H_{pq} = H_{qp}$ .

## 2.1. Analytical Modal Analysis

There are three different presentations for analytical model for the dynamic system. First one is the spatial model which is represented with the mass matrix, stiffness matrix, and damping matrix. Second one is the modal model which requires the modal parameters such as eigenfrequencies, mode shapes and damping ratios. The last one is the response model in the forms of Frequency Response Function (FRF) or Impulse Response Function (IRF). These models can represent the analytical Multi Input Multi Output (MIMO) model.

These three models are different in presentation, but related to each other. The interrelations are showed in figure 2.1. Modal model can be acquired from the spatial model by solving the eigenvalue problem. The spatial model can be obtained from the modal model by doing the coordinate transformation. The response model is used in the modal parameter estimation, and can be obtained from both spatial model and modal model. The theories about getting response model in terms of FRF or IRF from spatial model and modal model are introduced and used to develop the MATLAB codes in Appendix A.1.

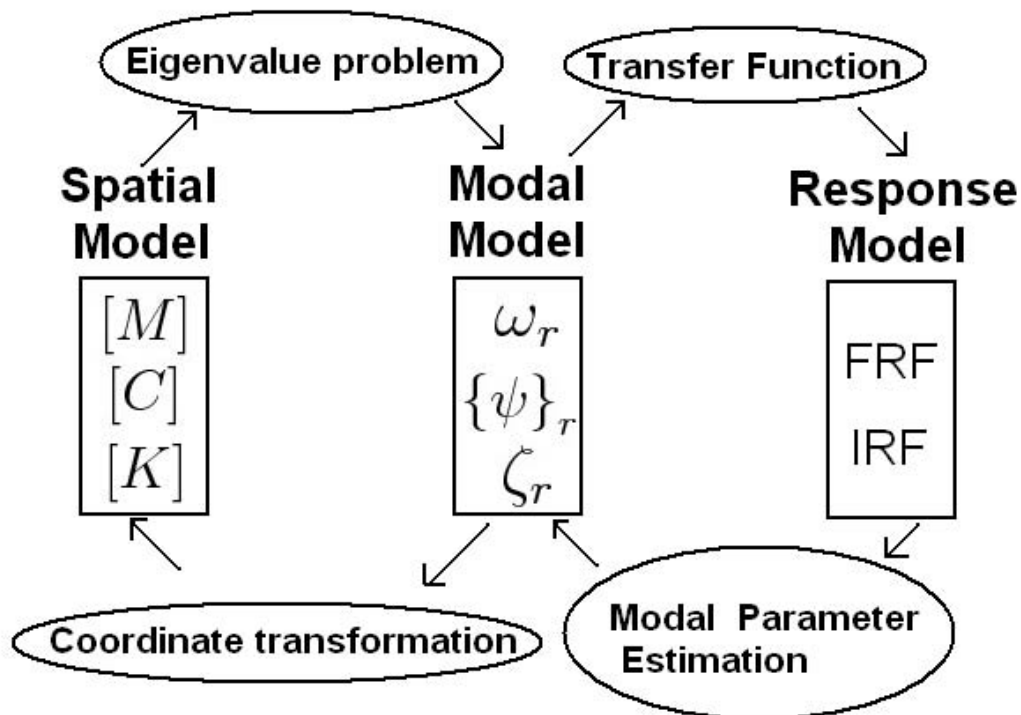


Figure 2.1.: Dynamic models interrelation

The detail of these theories can be found in reference[19] and pages 1 to 81 of

reference[15].

### 2.1.1. Spatial Model to Response Model

The first theory is about how to represent the modal shows in figure 2.2 into the response model. All the physical parameters of this MDOF model such as mass, damping and stiffness are provided. The equation of motion is also showed below in equation ( 2.1 ).

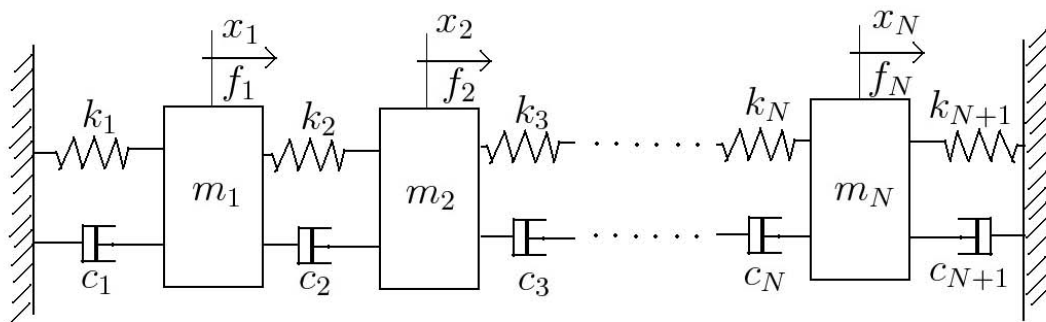


Figure 2.2.: Model with N degrees of freedom

Known:

Mass:  $m_1 \cdots m_N$

Damping:  $c_1 \cdots c_{N+1}$

Stiffness:  $k_1 \cdots k_{N+1}$

$$\begin{aligned}
 & \begin{bmatrix} m_1 & 0 & \cdots & 0 \\ 0 & m_2 & \cdots & 0 \\ \vdots & \vdots & \ddots & \vdots \\ 0 & 0 & \cdots & m_N \end{bmatrix} \begin{Bmatrix} \ddot{x}_1 \\ \ddot{x}_2 \\ \vdots \\ \ddot{x}_N \end{Bmatrix} \\
 + & \begin{bmatrix} c_1 + c_2 & -c_2 & \cdots & 0 \\ -c_2 & c_2 + c_3 & \cdots & 0 \\ \vdots & \vdots & \ddots & \vdots \\ 0 & 0 & \cdots & c_N + c_{N+1} \end{bmatrix} \begin{Bmatrix} \dot{x}_1 \\ \dot{x}_2 \\ \vdots \\ \dot{x}_N \end{Bmatrix} \\
 + & \begin{bmatrix} k_1 + k_2 & -k_2 & \cdots & 0 \\ -k_2 & k_2 + k_3 & \cdots & 0 \\ \vdots & \vdots & \ddots & \vdots \\ 0 & 0 & \cdots & k_N + k_{N+1} \end{bmatrix} \begin{Bmatrix} x_1 \\ x_2 \\ \vdots \\ x_N \end{Bmatrix} = \begin{Bmatrix} f_1 \\ f_2 \\ \vdots \\ f_N \end{Bmatrix} \quad (2.1)
 \end{aligned}$$

This can be written in the short form of equation ( 2.2 ).

$$[M] \{\ddot{\mathbf{x}}\} + [C] \{\dot{\mathbf{x}}\} + [K] \{\mathbf{x}\} = \{\mathbf{f}\} \quad (2.2)$$

Where  $[M]$  is mass matrix,  $[C]$  is damping matrix,  $[K]$  is stiffness matrix,  $\{\mathbf{f}\}$  is input force.

When the damping matrix  $[C]$  is non-proportional, the equations ( 2.2 ) of  $N$ -degree freedom system cannot yield the eigenvectors which can diagonalize the damping matrix. A technique can be used to solve this problem by reformulating the set of  $N$  equations into set of  $2N$  equations known as Hamilton's Canonical Equations [19]. Consequently, The reformulation must be applied for the general damping matrix  $[C]$ . The identity ( 2.3 ) will be take in consider.

$$[M] \{\dot{\mathbf{x}}\} - [M] \{\dot{\mathbf{x}}\} = 0 \quad (2.3)$$

Combine equations ( 2.2 ) and ( 2.3 ) yield a new system of  $2N$  equations.

$$[A] \{\dot{\mathbf{y}}\} + [B] \{\mathbf{y}\} = \{\bar{\mathbf{f}}\} \quad (2.4)$$

Where

$$[A] = \begin{bmatrix} [0] & [M] \\ [M] & [C] \end{bmatrix} \quad [B] = \begin{bmatrix} -[M] & [0] \\ [0] & [K] \end{bmatrix} \quad (2.5)$$

$$\{\dot{\mathbf{y}}\} = \begin{Bmatrix} \{\ddot{\mathbf{x}}\} \\ \{\dot{\mathbf{x}}\} \end{Bmatrix} \quad \{\mathbf{y}\} = \begin{Bmatrix} \{\dot{\mathbf{x}}\} \\ \{\mathbf{x}\} \end{Bmatrix} \quad \{\bar{\mathbf{f}}\} = \begin{Bmatrix} \{0\} \\ \{\mathbf{f}\} \end{Bmatrix}$$

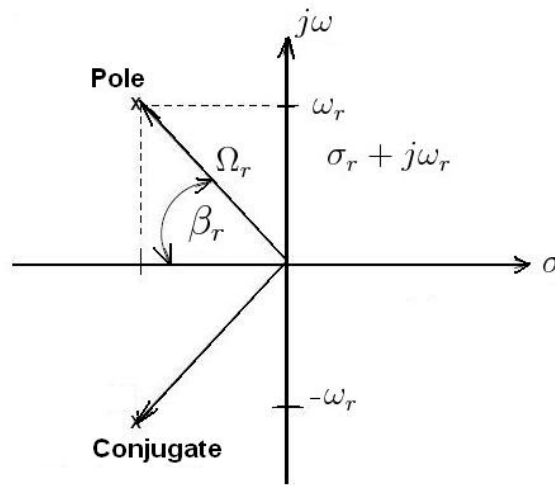


Figure 2.3.: Laplace plane pole location[19]

Note that all matrices in equation ( 2.4) are symmetric and this equation is now in a classical eigenvalue solution form. For this method, after solving the eigenvalue problem and obtaining the poles of the system, The eigenfrequencies and damping ratios can be calculated using the equations ( 2.7 ) ( 2.8 ). The locations of ploe are showed in the figure 2.3 and the notations used in the figure can be found following.

$\sigma_r$  : damping coefficient

$\omega_r$  : damped natural frequency

$\Omega_r$  : resonant (undamped natural frequency)

$\zeta_r = \cos \beta_r$  : damping factor (or percent of critical damping)

The pole  $\lambda_r$  cay be written as

$$\lambda_r = \sigma_r + j\omega_r = \left( -\zeta_r + j\sqrt{1 - \zeta_r^2} \right) \Omega_r \quad (2.6)$$

From the above relationship, the following equations can be derived. damping ratio:

$$\zeta_r = \frac{-\sigma_r}{\sqrt{\omega_r^2 + \sigma_r^2}} \quad (2.7)$$

damped natural frequency:

$$f_r = \frac{\omega_r}{2\pi} \quad (2.8)$$

And for the  $2N$  equation of system, we will use  $\{\varphi\}$  as the eigenvector. Notation  $\{\psi\}$  is used for eigenvector of the original  $N$  equation system.

$$[\varphi] = \left[ \begin{array}{cccccc} \{\varphi_1\} & \{\varphi_2\} & \{\cdots\} & \{\varphi_r\} & \{\cdots\} & \{\varphi_{2N}\} \end{array} \right] \quad (2.9)$$

$$[\varphi] = \left[ \begin{array}{cccccc} \lambda_1 \{\psi\}_1 & \lambda_2 \{\psi\}_2 & \cdots & \lambda_r \{\psi\}_r & \cdots & \lambda_{2N} \{\psi\}_{2N} \\ \{\psi\}_1 & \{\psi\}_2 & \cdots & \{\psi\}_r & \cdots & \{\psi\}_{2N} \end{array} \right] \quad (2.10)$$

Modal A is used for the theoretical case of damped systems (non-proportional or proportional), the modal A scaling factor is also the basis for the relationship between the scaled modal vectors and the residues determined from the measured frequency response functions. In general, for most experimental work, modal A is used as the default scaling approach. Starting with the analytical definition of modal mass in  $2N$  space.

$$\begin{aligned} M_{A_r} &= \{\varphi\}_r^T \left[ \begin{array}{cc} [0] & [M] \\ [M] & [C] \end{array} \right] \{\varphi\}_r \\ &= \left\{ \begin{array}{c} \lambda_r \{\psi\}_r \\ \{\psi\}_r \end{array} \right\}^T \left[ \begin{array}{cc} [0] & [M] \\ [M] & [C] \end{array} \right] \left\{ \begin{array}{c} \lambda_r \{\psi\}_r \\ \{\psi\}_r \end{array} \right\} \end{aligned} \quad (2.11)$$

Multiplying Equation ( 2.11 ) out in terms of space yields:

$$\begin{aligned} M_{A_r} &= \lambda_r \{\psi\}_r^T [M] \{\psi\}_r + \lambda_r \{\psi\}_r^T [M] \{\psi\}_r + \{\psi\}_r^T [C] \{\psi\}_r \\ &= \lambda_r M_r + \lambda_r M_r + C_r = 2\lambda_r M_r + C_r \end{aligned} \quad (2.12)$$

Applying the SDOF relationship between the modal damping and modal mass,

$$\begin{aligned} C_r &= -\sigma_r M_r \Rightarrow M_{A_r} = 2\lambda_r M_r - 2\sigma_r M_r \\ M_{A_r} &= 2(\sigma_r + j\omega_r) M_r - 2\sigma_r M_r = j2\omega_r M_r \end{aligned} \quad (2.13)$$

where  $M_{A_r}$  refers to modal A for mode  $r$ ;  $M_r$  is modal mass for mode  $r$ . From relationship between modal mass  $M_r$  and scaling factor  $Q_r$ , The relationship between  $M_{A_r}$  and  $Q_r$  in Equation ( 2.14 ) can be obtained.

$$M_r = \frac{1}{j2\omega_r Q_r} \Rightarrow M_{A_r} = \frac{1}{Q_r} \quad (2.14)$$

Then the residue  $A_{pqr}$  is

$$A_{pqr} = Q_r \psi_{pr} \psi_{qr} \quad (2.15)$$

Finally, The Frequency Response Function (FRF) and Impulse Response Function (IRF) with the relation in equation ( 2.16 ) can be derived.

$$\begin{aligned} H_{pq}(\omega) &= \sum_{r=1}^N \frac{A_{pqr}}{j\omega - \lambda_r} + \frac{A_{pqr}^*}{j\omega - \lambda_r^*} \\ h_{pq}(t) &= \sum_{r=1}^N A_{pqr} e^{\lambda_r t} + A_{pqr}^* e^{\lambda_r^* t} \end{aligned} \quad (2.16)$$

### 2.1.2. Modal Model to Response Model

The second theory is about how to represent the modal model into the response model. All the modal parameters of this MDOF model such as eigenfrequencies, modal damping ratios and the mode shapes in the terms of eigenvectors are provided.

Known:

Eigenfrequency for mode  $r$ :  $\omega_r = 2\pi f_r$  ;

Modal damping ration for mode  $r$ :  $\zeta_r$  ;

Scaled eigenvector for mode  $r$ :  $\{\psi\}_r$  ;

Residue for response location p, reference location q, for mode  $r$ :  $A_{pq}$  ;

We know the transfer function of the multi degree of freedom system as

$$H_{pq}(s) = \sum_{r=1}^N \frac{A_{pqr}}{s - \lambda_r} + \frac{A_{pqr}^*}{s - \lambda_r^*} \quad (2.17)$$

where  $H_{pq}$  is transfer function for response location p, reference location q;  $N$  refers to the number of modes;  $\lambda_r$  is  $r^{th}$  system eigenvalue or system pole;  $s$  is Laplace domain variable.

The  $H_{pq}(s)$  can be defined as  $H_{pq}(s) = \frac{X_p(s)}{F_q(s)}$  (2.18)

Therefore

$$X_p(s) = F_q(s) \sum_{r=1}^N \frac{A_{pqr}}{s - \lambda_r} + \frac{A_{pqr}^*}{s - \lambda_{pqr}^*} \quad (2.19)$$

The impulse excitation force will be unity after the Laplace transformation. So we can say  $F_q(s) = 1$ .

$$h_{pq}(t) = L^{-1} X_p(s) = L^{-1} \sum_{r=1}^N \frac{A_{pqr}}{s - \lambda_r} + \frac{A_{pqr}^*}{s - \lambda_{pqr}^*} = \sum_{r=1}^N A_{pqr} e^{\lambda_r t} + A_{pqr}^* e^{\lambda_{pqr}^* t} \quad (2.20)$$

Where  $h_{pq}(t)$  refers to impulse response function for response location p, reference location q.

From the figure 2.3, the following equation can be derived.

$$\lambda_r = \sigma_r + j\omega_r \quad (2.21)$$

$$\lambda_r = \sigma_r - j\omega_r \quad (2.22)$$

Where  $\sigma_r$  refers to real part of the system pole, or damping for mode  $r$ .

And then, the equation as following is defined

$$A_{pqr} = \frac{R_{pqr}}{2j} \quad (2.23)$$

Using Euler's formula, equation ( 2.20 ) becomes

$$\begin{aligned} h_{pq}(t) &= \sum_{r=1}^N \frac{R_{pqr}}{2j} [e^{(\sigma_r + j\omega_r)t} - e^{(\sigma_r - j\omega_r)t}] \\ &= \sum_{r=1}^N R_{pqr} e^{\sigma_r t} \frac{(e^{j\omega_r t} - e^{-j\omega_r t})}{2j} \\ &= \sum_{r=1}^N R_{pqr} e^{\sigma_r t} \sin(\omega_r t) \end{aligned} \quad (2.24)$$

The residues can be obtained from the known mode shapes.

$$[A]_r = Q_r \{\psi\}_r \{\psi\}_r^T \Rightarrow A_{pqr} = Q_r \psi_{pr} \psi_{qr} \quad (2.25)$$

where  $Q_r$  is constant which is scaling factor. The  $Q_r$  can be determined as following

$$Q_r = \frac{1}{2j\omega_r M_r} \quad (2.26)$$

Equation ( 2.26 ) represents the relationship between modal mass and the scaling involved between the residues and the modal vectors. Therefore, once the residue information is found for mode  $r$  and some convenient form of modal vector scaling is

chosen for mode  $r$ , the scaling constant can be determined. Equation ( 2.26 ) can be used to determine modal mass for mode  $r$  consistent with the modal vector scaling.

These theories discussed above are used to develop the MATLAB code which is used to create several analytical data sets in the form of response model from both modal model and spatial model to verify the modal parameter estimation methods. And this part is also the fundamentals of experimental modal analysis.

## 2.2. Experimental Modal Analysis

Experimental modal analysis is an experimental approach to determine the modal parameters (eigenfrequencies, damping factors, modal vectors and modal scaling) of a system under the assumptions established in the beginning of the Chapter. The modal parameters determined experimentally serve for future evaluations such as structural modifications. Experimental modal analysis is used to explain dynamic problems such as vibration or acoustic that is not obvious from the analytical models. It is important to remember that most vibration and acoustic problems are a function of both the forcing functions (or initial conditions) and the system characteristics described by the modal parameters [20]. As a result, the experimental modal analysis can be summarized as two steps: Experimental Data Acquisition and Data Processing.

The detail of the experimental modal analysis can be found in reference [15] and reference [20]. Here the details about the theories related to experiment and modal parameter estimation methods are presented.

### 2.2.1. Experiment Process

- Discretize structure and define nodes
- Either use roving sensor(s) (and fixed actuator(s)) Or roving actuator(s) (and fixed sensor(s))
- Excite the structure using impact hammer or shaker as actuator
- Measurement of all input and output signals
- Calculate frequency response function (FRF)
- Perform modal parameter estimation from acquired FRF signals



### 2.2.2. Modal Parameter Estimation Methods

In this section, the modal parameter estimation methods are introduced and classified. A brief description of some methods that used in software X-Modal II are discussed. The details of these methods can be found in reference [15], reference [20], reference [1] and reference [10].

The methods can be classified into time domain and frequency domain methods. Time domain and frequency domain methods can be divided into indirect (or modal) and direct methods. The former means the identification of the FRF is based on the modal model. The latter means that the identification is directly based on the spatial model. A further division concerns the number of modes that can be analyzed. In this respect, Single degree-of-freedom and Multi degree-of-freedom analyses can be classified. In time domain only MDOF analysis can be applied. Direct methods only apply to MDOF analysis. The figure 2.4 shows a diagram with the various possible categories of methods.

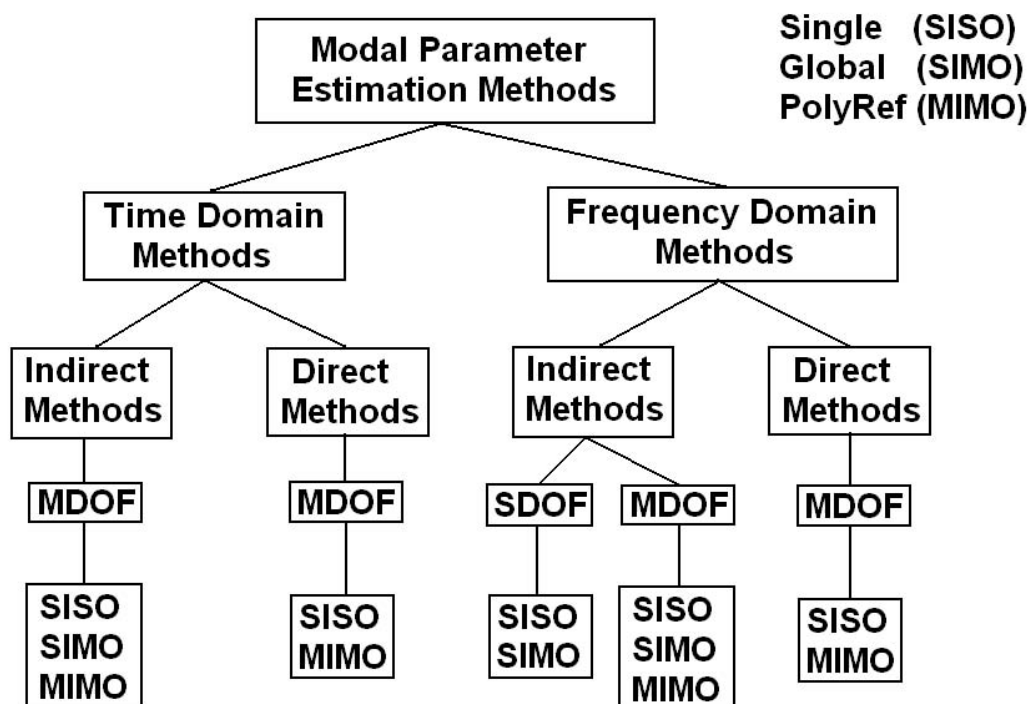


Figure 2.4.: Classification of modal analysis methods[15]

Here, we will provide a brief introduction of the theories of the methods used in the X-Modal II, which are PTD, ERA, RFP, PFD and RFP-z.

### The Polyreference Time Domain (PTD)

The PTD method is a time domain, indirect, high order, MIMO method. The PTD method, which is also called as Polyreference complex exponential method, is an extension of the Least squares complex exponential method (LSCE). This method can both estimate any part of the modal vector in their solutions for the modal frequencies and indicate the existence of repeated roots. Since this algorithm has good numerical characteristics, it is still the most commonly used algorithms today. The only limitation is the cases involving high damping. As a high order algorithm, more time domain information is required compared to the low order algorithm.

The basic equation is

$$\begin{aligned} \left[ \begin{array}{cccc} [h(t_{i+0})] & [h(t_{i+1})] & \cdots & h(t_{i+m-1}) \end{array} \right]_{N_o \times N_i m} \begin{bmatrix} [\alpha_0] \\ [\alpha_1] \\ \cdots \\ [\alpha_{m-1}] \end{bmatrix}_{N_i m \times N_i} \\ = - [h(t_{i+m})]_{N_o \times N_i} \end{aligned} \quad (2.27)$$

One way to estimate the modal frequencies and modal vectors in the PTD algorithm is to use a companion matrix, a state-space reduction of a high order matrix equation to many first order matrix equations. The companion form is advantageous as an eigenvalue decomposition of the companion matrix generates the modal frequencies and modal vectors in one step. When the inputs are the references, the modal vectors are filled with modal participation factors.

$$\begin{aligned} \left[ \begin{array}{ccccc} -[\alpha_{m-1}] & -[\alpha_{m-2}] & \cdots & -[\alpha_1] & -[\alpha_0] \\ [I] & [0] & \cdots & [0] & [0] \\ \vdots & \vdots & \cdots & \vdots & \vdots \\ [0] & [0] & \cdots & [I] & [0] \end{array} \right]_{(N_i m \times N_i) \times (N_i m \times N_i)} \begin{bmatrix} \{z_{m-1}\} \\ \{z_{m-2}\} \\ \vdots \\ \{z_0\} \end{bmatrix}_{N_i m \times N_i} = \lambda \begin{bmatrix} \{z_{m-1}\} \\ \{z_{m-2}\} \\ \vdots \\ \{z_0\} \end{bmatrix}_{N_i m \times N_i} \end{aligned} \quad (2.28)$$

We can convert  $z_r$  to  $\lambda_r$  use the relationship showed in equation (2.29).

$$\begin{aligned} z_r &= e^{\lambda_r \Delta t} & \lambda_r &= \sigma_r + j\omega_r \\ \sigma_r &= \text{Re} \left[ \frac{\ln z_r}{\Delta t} \right] & \omega_r &= \text{Im} \left[ \frac{\ln z_r}{\Delta t} \right] \end{aligned} \quad (2.29)$$

The necessary steps to use the present method are as follows: first, to take all the time records of the IRFs to enter in the basic equation ( 2.27 ) and solve it; second, to calculate the eigenvalues and eigenvectors of the companion matrix equation ( 2.28 ) in order to find the natural frequencies and damping factors; finally to calculate the residues.

This method can determine the multiple roots or closely spaced modes of a structure. The time required for the analysis is reduced and the accuracy in the results increased. It has also shown some difficulties in analyzing satisfactorily structures with high damping.

### The Eigensystem Realization Algorithm (ERA)

The ERA method is a time domain, indirect, first order, MIMO method. It is simply a multiple reference version of the Ibrahim time domain (ITD) algorithm. This algorithm is essentially a state-space formulation with respect to the second order time domain algorithms.

The basic equation is

$$[[h(t_{i+0})] [h(t_{i+1})]]_{N_i \times 2N_o} [[\alpha_0]]_{2N_o \times 2N_o} = - [[h(t_{i+1})] [h(t_{i+2})]]_{N_i \times 2N_o} \quad (2.30)$$

The Hankel matrix is showed in equation ( 2.31 ) which is formed by the Markov parameters is showed in equation ( 2.32 ).

$$[H(k-1)] = \begin{bmatrix} [X(k)] & [X(k+1)] & \cdots & [X(k+j)] \\ [X(k+1)] & [X(k+2)] & \cdots & [X(k+j+1)] \\ \vdots & \vdots & \cdots & \vdots \\ [X(k+i)] & [X(k+i+1)] & \cdots & [X(k+i+j)] \end{bmatrix} \quad (2.31)$$

$$[X(k)] = [R] [A]^{k-1} [B] \quad (2.32)$$

where

$$\begin{aligned} \{x(t)\} &= [R] \{u(t)\} \\ [A] &= e^{[A']\Delta t} \\ [B] &= \int_0^{\Delta t} e^{[A']\tau'} d\tau' [B'] \end{aligned} \quad [A'] = \begin{bmatrix} [0] & [I] \\ -[M]^{-1}[K] & -[M]^{-1}[C] \end{bmatrix} \quad [B'] = \begin{bmatrix} [0] \\ [M]^{-1}[F] \end{bmatrix} \quad (2.33)$$

The pseudo-inverse of  $[H(0)]$  can be calculated via the Singular Value Decomposition (SVD).

$$[H(0)] = [U] [\Sigma] [V]^T \quad (2.34)$$

Calculate the realized matrices with the equation ( 2.35 ).

$$\begin{aligned} [R] &= [E_p]^T [U_{2N}] [\Sigma_{2N}]^{1/2} \\ [A] &= [\Sigma_{2N}]^{-1/2} [U_{2N}]^T [H(1)] [V_{2N}] [\Sigma_{2N}]^{1/2} \\ [B] &= [\Sigma_{2N}]^{1/2} [V_{2N}]^T [E_q] \end{aligned} \quad (2.35)$$

$$\text{where } [E_p]^T = \begin{bmatrix} [I] & [0] & \cdots & [0] \end{bmatrix} \quad [E_q] = \begin{bmatrix} [I] \\ [0] \\ \vdots \\ [0] \end{bmatrix}$$

In order to determine the modal parameters of the system, we must solve the eigenproblem based on the  $[A]$ , of the form of the equation ( 2.36 ).

$$[A] \{ \psi_u \} = \lambda \{ \psi_u \} \quad (2.36)$$

The mode shape in terms of physical coordinates of the system is showed in equation ( 2.37 )

$$\{ \psi_x \} = [R] \{ \psi_u \} \quad (2.37)$$

The relationship between eigenvalues  $\beta_r + i\gamma_r$  and the roots of the system  $s_r = a_r + ib_r$  is used to calculate the damping ratios and natural frequencies with the equation ( 2.38 )

$$\beta_r + i\gamma_r = e^{(a_r + ib_r)\Delta t} = V_r \quad R_r = \text{In}(V_r) \quad f_r = \frac{|R_r|}{2\pi \cdot \Delta t} \quad \xi_r = \sqrt{\frac{1}{1 + \left(\frac{\text{Im}(R_r)}{\text{Re}(R_r)}\right)^2}} \quad (2.38)$$

The necessary step to perform an analysis with the ERA are as follows: first, choice of the measured data to construct matrix  $[H(0)]$ ; second, calculate of the SVD of  $[H(0)]$ , to calculate  $[U_{2N}]$ ,  $[V_{2N}]$  and  $[\Sigma_{2N}]$  and to recalculate  $[H(0)]$  based on the value of the rank found (order of the system); third, construction of matrix  $[H(1)]$  and calculation of the 'realized' matrices  $[R]$ ,  $[A]$  and  $[B]$ ; at last, calculation of the eigenvalues and eigenvectors of matrix  $[A]$  and the eigenvectors corresponding to the physical coordinates and calculation of the modal parameters.

This method, as the results from the SVD, may not be correct when there are noise or nonlinearities.

### The Rational Fraction Polynomial Method (RFP)

The RFP method is a frequency domain, indirect, high order, SISO method. The formulation of the FRF is expressed in rational fraction form equation ( 2.39 ) instead of the partial fraction form where the error function is established in a way that the resulting system of equations is linear. Because the resulting linear system of equations involves matrices that are ill conditioned, the Gradient Method is used to minimize this error function and initial estimate is calculated by using the least Square Method [10].

$$H(\omega) = \frac{\sum_{k=0}^{2N-1} a_k (i\omega)^k}{\sum_{k=0}^{2N} b_k (i\omega)^k} \quad (2.39)$$

Set  $b_{2N} = 1$ , this leads to

$$e'_j = \sum_{k=0}^{2N-1} a_k (i\omega_j)^k - H_e(\omega_j) \left[ \sum_{k=0}^{2N-1} b_k (i\omega_j)^k + (i\omega_j)^{2N} \right] \quad (2.40)$$

The error function is showed in equation ( 2.41 ) and ( 2.42 ).

$$[E] = \begin{bmatrix} 1 & (i\omega_1) & (i\omega_1)^2 & \cdots & (i\omega_1)^{2N-1} \\ 1 & (i\omega_2) & (i\omega_2)^2 & \cdots & (i\omega_2)^{2N-1} \\ \vdots & \vdots & \vdots & \ddots & \vdots \\ 1 & (i\omega_L) & (i\omega_L)^2 & \cdots & (i\omega_L)^{2N-1} \end{bmatrix} \begin{Bmatrix} a_0 \\ a_1 \\ \vdots \\ a_{2N-1} \end{Bmatrix} - \begin{Bmatrix} H_e(\omega_1) (i\omega_1)^{2N} \\ H_e(\omega_2) (i\omega_2)^{2N} \\ \vdots \\ H_e(\omega_L) (i\omega_L)^{2N} \end{Bmatrix} \\ - \begin{bmatrix} H_e(\omega_1) & H_e(\omega_1) (i\omega_1) & \cdots & H_e(\omega_1) (i\omega_1)^{2N-1} \\ H_e(\omega_2) & H_e(\omega_2) (i\omega_2) & \cdots & H_e(\omega_2) (i\omega_2)^{2N-1} \\ \vdots & \vdots & \ddots & \vdots \\ H_e(\omega_L) & H_e(\omega_L) (i\omega_L) & \cdots & H_e(\omega_L) (i\omega_L)^{2N-1} \end{bmatrix} \begin{Bmatrix} b_0 \\ b_1 \\ \vdots \\ b_{2N-1} \end{Bmatrix} \quad (2.41)$$

$$\{E\} = [P] \{a\} - [T] \{b\} - \{W\} \quad (2.42)$$

The squared error function  $J$  will be minimized with the Gradient method.

$$J = \{E^*\}^T \{E\} \quad (2.43)$$

After minimize equation ( 2.43 ) using the Gradient method, we can get the coefficients of the rational fraction equation ( 2.39 ). Then the roots or poles of the denominator polynomial contain the values of the natural frequency and damping ratio. These can be obtained with equation ( 2.44 ).

$$f_r = \frac{|s_r|}{2\pi} \quad \xi_r = -\frac{\text{Re}(s_r)}{|s_r|} \quad (2.44)$$

This high order frequency domain algorithm, in the form of scalar coefficients, was the multiple degree of freedom algorithm utilized to estimate modal parameters once discrete data was available. The algorithm works well for narrow frequency bands and limited numbers of modes but have poor numerical characteristics otherwise. While the use of multiple references reduces the numerical conditioning problem, the problem is still significant and not easily handled. In order to circumvent the poor numerical characteristics, many approaches have been used (frequency normalization, orthogonal polynomials) but the use of low order frequency domain models has proven more effective.

### The Polyreference Frequency Domain method (PFD)

The PFD method is a frequency domain, indirect, second order, MIMO method. The basic equation for this method is showed in equation ( 2.45 ).

$$\begin{aligned} \left[ \begin{array}{cccc} [H(\omega_i)] & (j\omega_i)^1 [H(\omega_i)] & -[I] & -(j\omega_i)[I] \end{array} \right]_{N_i \times 4N_o} \begin{bmatrix} [\alpha_0] \\ [\alpha_1] \\ [\beta_0] \\ [\beta_1] \end{bmatrix}_{4N_o \times N_o} \\ = - (j\omega_i)^2 [H(\omega_i)]_{N_i \times N_o} \end{aligned} \quad (2.45)$$

This method given evidence of good performance when dealing with close modes; it appears also be less sensitive to computational modes when compared to time domain methods and allows for the use of unequal frequency step.

This algorithm has superior numerical characteristics compared to the high order frequency domain algorithms. Unlike the low order time domain algorithms, though, sufficient data from across the complete frequency range of interest must be included in order to obtain a satisfactory solution.

### The RFP-z method

There was several different names for this method such as PolyMax method. This method is a polyreference least square complex frequency domain MIMO method. It can be implemented simliarly as PTD method. The necessary step to perform an analysis with the RFP-z are as follows: First, represent the measured FRFs with the right matrix fraction model which showed in the equation ( 2.46 ).

$$[H(\omega)] = \sum_{r=0}^p z^r [\beta_r] \left( \sum_{r=0}^p z^r [\alpha_r] \right)^{-1} \quad (2.46)$$

where  $[H(\omega)]$  is matrix containing with the FRFs between all  $m$  input and all  $l$  output in the complex domain.  $[\beta_r]$  are the numerator matrix polynomial coefficients;  $[\alpha_r]$  are the denominator matrix polynomial coefficients.  $p$  is the model order. The model for the equation ( /refeqn:rmfm ) is called z-domain modal with

$$z = e^{j\omega\Delta t} \quad (2.47)$$

where  $\Delta t$  is the sampling time. The unknown model coefficients  $[\alpha_r]$ ,  $[\beta_r]$  are then found with the least square method. Second, after determin the denominator matrix polynomial coefficients. the poles and modal participation facors can be obtained from the eigensolution of the companion matrix [14] [12]. Third, here a new way to determine the mode shapes will be provided with a model named pole-residue model [14]

[12]. the mode shapes can be obtained by solving the pole-residue model with the linear least square method.

The advantage is that, the method will yields very clear consistency diagram than other method, in other words, it is easy to the physical poles from the diagram. This is because the non-physical poles will be estimated with negative damping ratio so that the diagram only contains the physical poles. And this method can deal with large frequency range and large model order, since it does not suffer from the numerical problems as it is in the z-domain. The method shows very good performance for the systems with high damping ratios [12].

### 2.2.3. Universal File Format (UFF)

The experimental data collected from the experiment is stored in UFF files. The detail format can be found on the website of UC-SDRC and reference [25].

Universal File Formats (UFF) were originally developed by the Structural Dynamics Research Corporation (SDRC) in the late 1960s and early 1970s to facilitate data transfer between Computer Aided Design (CAD) and Computer Aided Test (CAT) in order to make the Computer Aided Engineering (CAE) easier. SDRC continues to support and use the UFF as part of their CAE software.

The formats were originally developed as 80 character in each line, ASCII records that occur in a specific order according to each UFF. As computer files became routinely available, single UFF were concatenated into computer file structures. Recently, a hybrid UF file structure (UF Dataset 58 Binary) was developed. The data stored in this format is twice as small as the former format.

The use of the Universal File Format as a "standard" has been of great value to the experimental dynamics (vibration and acoustic) community, particularly in the area of modal analysis.

## 2.3. FE Simulation

The details of this part can be found on the reference [23], reference [9], reference [11] and reference [4].

The joint connections can be divided into normally loaded and tangentially loaded joints. Generally, the damping in normally loaded joints is very small compared to tangentially loaded since the relative displacement of the two parts of the joint is the main factor which influence the damping and there will be relatively small displacement in the normal direction [9].

It has been shown by experimental investigations that joint damping is nearly frequency independent. Similar results have been shown for material damping in metals, where the main cause of dissipation is inner friction in the material [23]. During the FE modeling the constant hysteresis damping will be used. The method uses frequency-independent damping and linear joint stiffness parameters in order to predict the vibration response of structures. This allows fast prediction of the eigenfrequencies and modal damping factors of structures before there exists a physical prototype for experimental testing [9].

The thin-layer element is a method making use of thin layer elements for interfaces and joints. The basic idea is that the behavior near the interface involves a finite thin zone. The response of that zone is different from the behavior of the surrounding materials and it is achieved by considering appropriate constitutive law for the element [7].

During the calculation of the vibrational characteristics of the structure with the FEM, the following equation of motion for an undamped system is used.

$$[M] \{\ddot{u}\} + [K] \{u\} = \{0\} \quad (2.48)$$

Where  $[M]$  is a mass matrix,  $[K]$  is a real valued stiffness matrix, and  $\{u\}$  is the displacement vector. Eigenvalues and eigenmodes can be determined by performing a numerical modal analysis with ANSYS. For the case of utilizing constant hysteresis damping, it will be add to the stiffness matrix as a complex-valued product of dissipation multiplier  $\alpha_i$  and  $\beta_i$  for the material and the joint damping.

$$[K^*] = [K] + j[C] = [K] + j \sum_{i=1}^n \alpha_i [K_i^{material}] + j \sum_{i=1}^n \beta_i [K_j^{joint}] \quad (2.49)$$

where for the considered system with low damping  $\alpha_i, \beta_i \ll 1$ , this problem can be solved by harmonic analysis in ANSYS. And in this case modal damping for the structure can be estimated from the FRF obtained from the harmonic analysis.

Simulating with ANSYS, The damping matrix  $[C]$  is used in harmonic analyses. In its most general form, it is showed in equation ( 2.50 ). The detail of this part can be found in reference [11] and reference [4]

$$[C] = \alpha [M] + (\beta + \beta_c) [K] + \sum_{j=1}^{N_m} \left[ \left( \beta_j^m + \frac{2}{\Omega} \beta_j^\xi \right) [K_j] \right] + \sum_{k=1}^{N_e} [C_k] + [C_\xi] \quad (2.50)$$

where

$[C]$  = structure damping matrix

$\alpha$  = mass matrix multiplier (input on ALPHAD command)



$[M]$  = structure mass matrix

$\beta$  = stiffness matrix multiplier (input on BETAD command)

$\beta_c$  = variable stiffness matrix multiplier

$[K]$  = structure stiffness matrix

$N_m$  = number of materials with DAMP or DMPR input

$\beta_j^m$  = stiffness matrix multiplier for material j (input as DAMP on MP command)

$\beta_j^\xi$  = constant (frequency-independent) stiffness matrix coefficient for material j  
(input as DMPR on MP command)

$\Omega$  = circular excitation frequency

$K_j$  = portion of structure stiffness matrix based on material j

$N_e$  = number of elements with specified damping

$C_k$  = element damping matrix

$C_\xi$  = frequency-dependent damping matrix

For the simulation,  $\alpha$  and the  $\beta_j^\xi$  is related to complex-value stiffness coefficients  $\alpha_i$  and  $\beta_i$  in equation ( 2.49 ), since  $\beta_j^\xi$  is frequency-independent and can represent the damping of the material with constant constant hysteresis.

A Schematic diagram of an arbitrary joint modeled by a thin layer is presented in figure 2.5.

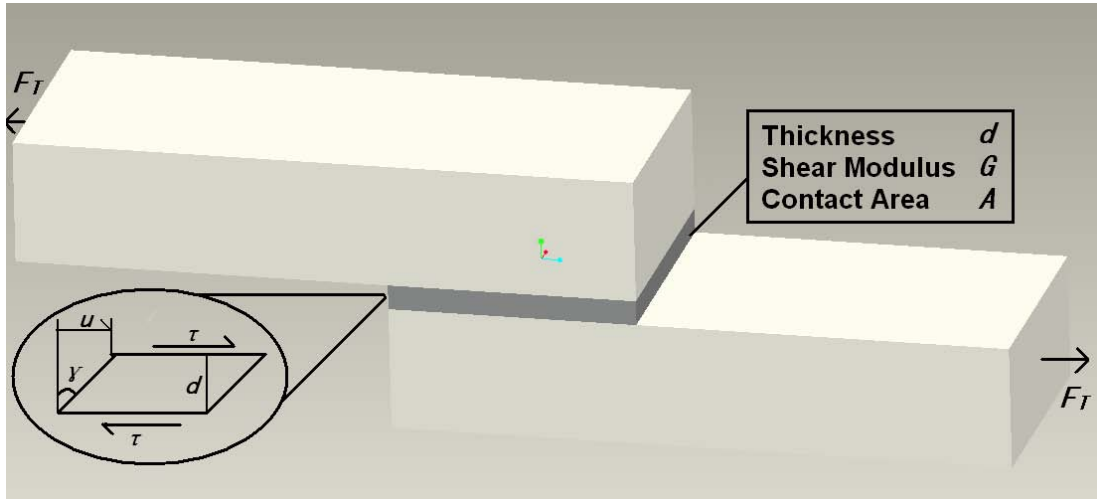


**Figure 2.5.:** Schematic diagram of a joint with a thin layer element

The stress can be expressed as

$$\tau = G\gamma \approx G\frac{u}{d} \quad (2.51)$$

where  $G$  is the shear modulus and  $\gamma$  is the shear angle. The shear stress can also be

estimated by the ratio of tangential force  $F$  and area of the contact  $A$ .

$$\tau = \frac{F}{A} \quad (2.52)$$

Combining Equations ( 2.51 ) and ( 2.52 ), the force can be calculated

$$F \approx \frac{GA}{d}u = ku \quad (2.53)$$

It is important to recognize that the characteristics of the joint's interface that is represented by the thin layer elements is orthotropic. There are significant differences in tangential and normal behavior of the joint

From equation ( 2.53 ) the shear modulus can be approximated as

$$G = \frac{kd}{A} \quad (2.54)$$

The damping coefficient  $\xi$  for the joint and stiffness  $k$  can be obtained from the joint patch experiment. The material damping can also be determined by experimental approach with half-width value method. The related experiments are introduced in reference [23]

For the simulation, the orthotropic material has been chosen and the constitutive material law can be expressed in the equation ( 2.55 ).

$$\begin{bmatrix} \sigma_{xx} \\ \sigma_{yy} \\ \sigma_{zz} \\ \sigma_{xy} \\ \sigma_{yz} \\ \sigma_{zx} \end{bmatrix} = \begin{bmatrix} E_{11} & E_{12} & E_{13} & 0 & 0 & 0 \\ & E_{22} & E_{23} & 0 & 0 & 0 \\ & & E_{33} & 0 & 0 & 0 \\ & & & E_{44} & 0 & 0 \\ & & & & E_{55} & 0 \\ & & & & & E_{66} \end{bmatrix} \begin{bmatrix} \varepsilon_{xx} \\ \varepsilon_{yy} \\ \varepsilon_{zz} \\ \varepsilon_{xy} \\ \varepsilon_{yz} \\ \varepsilon_{zx} \end{bmatrix} \quad (2.55)$$

The off-diagonal terms ( $E_{12}, E_{13}, E_{23}$ ) are zero for physical reasons (there is no transversal constriction invoked by the contact interface). Also, since the interface has no stiffness in and directions (parallel to the joint's surface), the terms  $E_{11}$  and  $E_{22}$  disappear.  $E_{33}$  represents the normal stiffness, whereas  $E_{55} = E_{66} = G$  define the tangential stiffness of the joint. Since the joint exhibits no stiffness for in-plane shearing,  $E_{44}$  is also zero. For numerical reasons all diagonal terms in equation ( 2.55 ) must be different from zero. Thus, in the calculation the values of  $E_{11}$ ,  $E_{22}$  and  $E_{44}$  are set to some small values.

And in this thesis, the interrelations between the joint characteristics and the material parameters such as shear module  $G$  and  $\beta_j^\xi$  will be figured out.

## 3. Design the System

For this thesis, design a mechanical system which can perform different joint properties is compulsory, in order to investigate the relationship between joint properties and the structural dynamic properties. In this chapter design and verification of a mechanical structure will be carried out with the help of ANSYS.

### 3.1. Criteria

There are several criteria need to be satisfied.

- The maximum mass of the total system is  $20kg$ . The mass must be big enough to avoid the massloading effect of the accelerometers or the bolts. however, it cannot be exceed the capability of experimenter as the structure must hanged during the experiment.
- The 1st eigenfrequency must between  $100Hz$  and  $400Hz$ . The eigenfrequencies of the strucutre supposed to be lies in the low frequency range.
- Different pressure distribution must be counted in. and this can be relized with different bolt spacing. In this thesis, the pressure distribution is one of the important factors need to be investigated which influence the dynamic properties of the structure.
- The structure must assembled in several different ways. This related to the capability of the structure to perform many different joint characteristics.
- The structure must as simple as possible. So that the problem will be simply described and the relations between the joint characteristics and dynamic properties of the structure can be clearly expressed.

## 3.2. Design

### 3.2.1. Assumption

Here, arbitrary structures and dimensions are given and checked with ANSYS, the structures need to satisfy the criteria discussed in section 3.1. The assumptions for the simulation with ANSYS must be made before design. First, the whole structure assumed to be welded together. Second, all parts has the same material properties as the eigenfrequency and modes shape did not depend too much on the damping properties. Under this two assumption the simulation will be carried out to verify whether the designed structure satisfies the criteria or not. The ANSYS command can be checked in reference [4]. and the command stream which used to set up the structure is showed in Appendix A.2.

### 3.2.2. Structure

After several times of simulation and redesign process, finally, the structure of system determined to be constructed with two separate parts, named structure B and structure C. The detail size, shape can be found in the Appendix A.3. The design of the shape of the structure, the joint and the ways of assembly can be referenced from the reference [8].

In this thesis, the Structure B and Structure C was used to form a structure with bolt which showed in figure 3.1.

With the structure designed, several different assemblies can be constructed and can also perform joints with different characteristics.

### 3.2.3. Simulation

The necessary steps for the simulation is: first, decide the mesh size for the following step; second, perform the modal analysis to check whether the structure satisfy the criteria or not. Mesh size affects the accuracy of the simulation. As the mesh size getting smaller, the finite elements model will tends to real model and the simulation results will approach the exact values.

#### Determine the Mesh Density

As the main structure which will create the major parts of the elements is Structure B, the influence that caused by the mesh size of this structure must be investigated. And here the structure A (figure 3.2 and Appendix A.3) designed and used to verify the

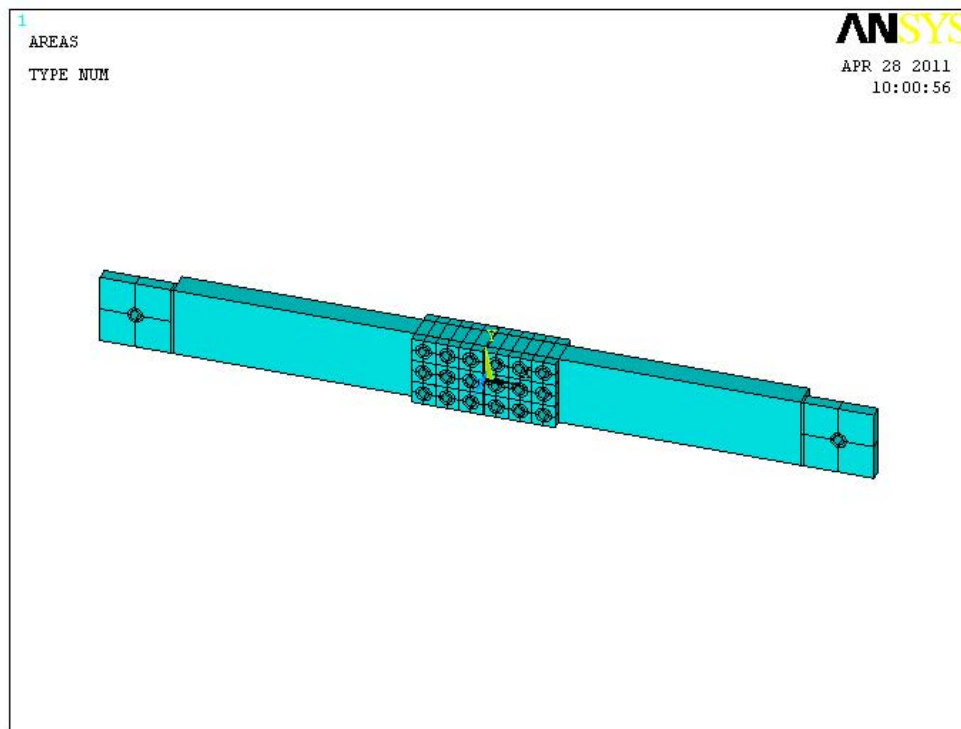


**Figure 3.1.:** Drawing of the assembled structure

influence of the mesh size as the example. As the mesh size getting smaller, the result

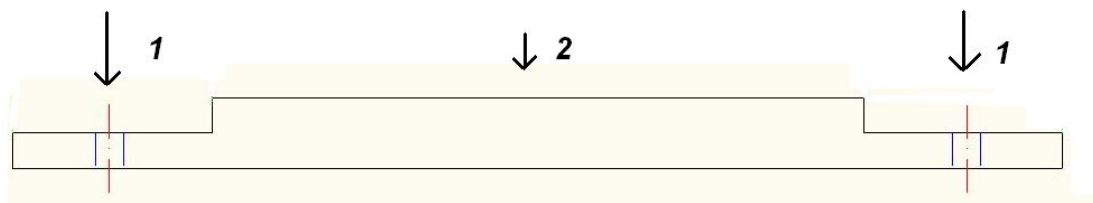


**Figure 3.2.:** Meshing the structure A

will be converge to a certain value. The relation between the mesh size and the result will be discussed in the following.

The mesh size over the both sides which will be conneted with other structure indicated 1 in the figure 3.2 must be small enough in order to represent with the effect of joint clearly. The mesh size over the middle part indicated 2 in the figure 3.2 of structure A can be changed as there will be less thing happens and the the influence of mesh size for this part will be not significant. As a result, the element numbers can be reduced. Comparing 4 different mesh sizes: First the division over length of part

2 is 76; second the division is 38; third the division is 19, at last, the division 13 is performed. The first three eigenfrequencies for each mesh size are compared. The Mass of this structure is 1.88554kg. and the result is showed below with the table 3.1 and figure 3.3.

**Table 3.1.:** Comparison with different meshing density

Division	Mesh Size(mm)	Eigenfrequencies(Hz)		
		1st	2nd	3rd
76	2.5	1216.8,	2411	3316.8
38	5	1218.1,	2417.4	3319.7
19	10	1221.1	2431.4	3327
13	14.615	1224.3	2444.9	3333.7

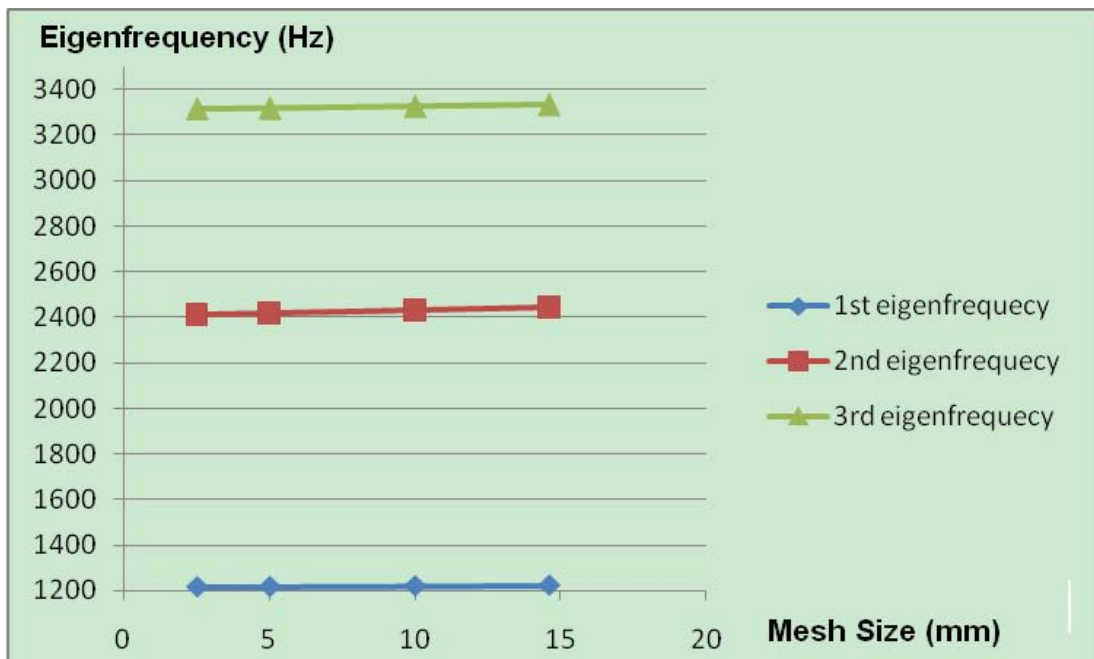


**Figure 3.3.:** Eigenfrequencies of the Structure with different Meshing density

- For division of 76. The length is 2.5mm and length width ratio of the element is 2.5:4.583. The first three eigenfrequencies are 1216.8Hz, 2411.0Hz and 3316.8Hz.
- For division of 38. The length is 5mm and length width ratio of the element is 5:4.583. The first two eigenfrequencies are 1218.1Hz, 2417.4Hz and 3319.7Hz.

- C. For division of 19. The length is 10mm and length width ratio of the element is 10:4.583. The first two eigenfrequencies are 1221.1Hz, 2431.4Hz and 3327.0Hz.
- For division of 13. The length is 14.615mm and length width ratio of the element is 14.615:4.583. The first two eigenfrequencies are 1224.3Hz, 2444.9Hz and 3333.7Hz.

The result can be found in the figure 3.3 that the mesh will not influence the result too much, and the division of 25 will be chosen in order to make sure not only the accuracy of the result, but also reduce the calculating time.

### Modal Analysis

After determining the mesh size and meshing the structure, the modal analysis with ANSYS will be carried out to calculate the eigenfrequencies of the assembly structure. Detail introduction of the modal analysis can be found in reference [3] and the command stream for modal analysis is showed in Appendix A.2.

The mode shapes and the eigenfrequencies for the first 8 modals are showed in figure 3.4.

### Comparison with the criteria

- Mass  
Here the density of all the structure is set to  $7800\text{kg}/\text{m}^3$  and the total mass for the structure showed in figure 3.1 is  $5\ 37043\text{kg}$ . The total mass is much smaller than  $20\text{kg}$  state in the criteria. This structure is easy to set up since the structure is not so heavy, but there will be some effect of massloading. At the following section 5.1, the massloading effect will be checked out, and it shows the effect of massloading is small enough to ignore.
- First three eigenfrequency  
When division is 25, element number is 30080, young's modulus is  $2\ 05e11$  and poisson's ratio is 0.3. then the results are: 1st mode is  $371\ 7\text{Hz}$ ; 2nd mode is  $811\ 7\text{Hz}$ ; 3rd mode is  $867\ 3\text{Hz}$ . This is satisfying the criterion for first eigenfrequency and the first several eigenfrequencies of this structure will lie in the low frequency range.
- The structure can perform different bolt spacing.  
The bolt holes of the joint designed into a  $3 \times 3$  array. With this structure, many

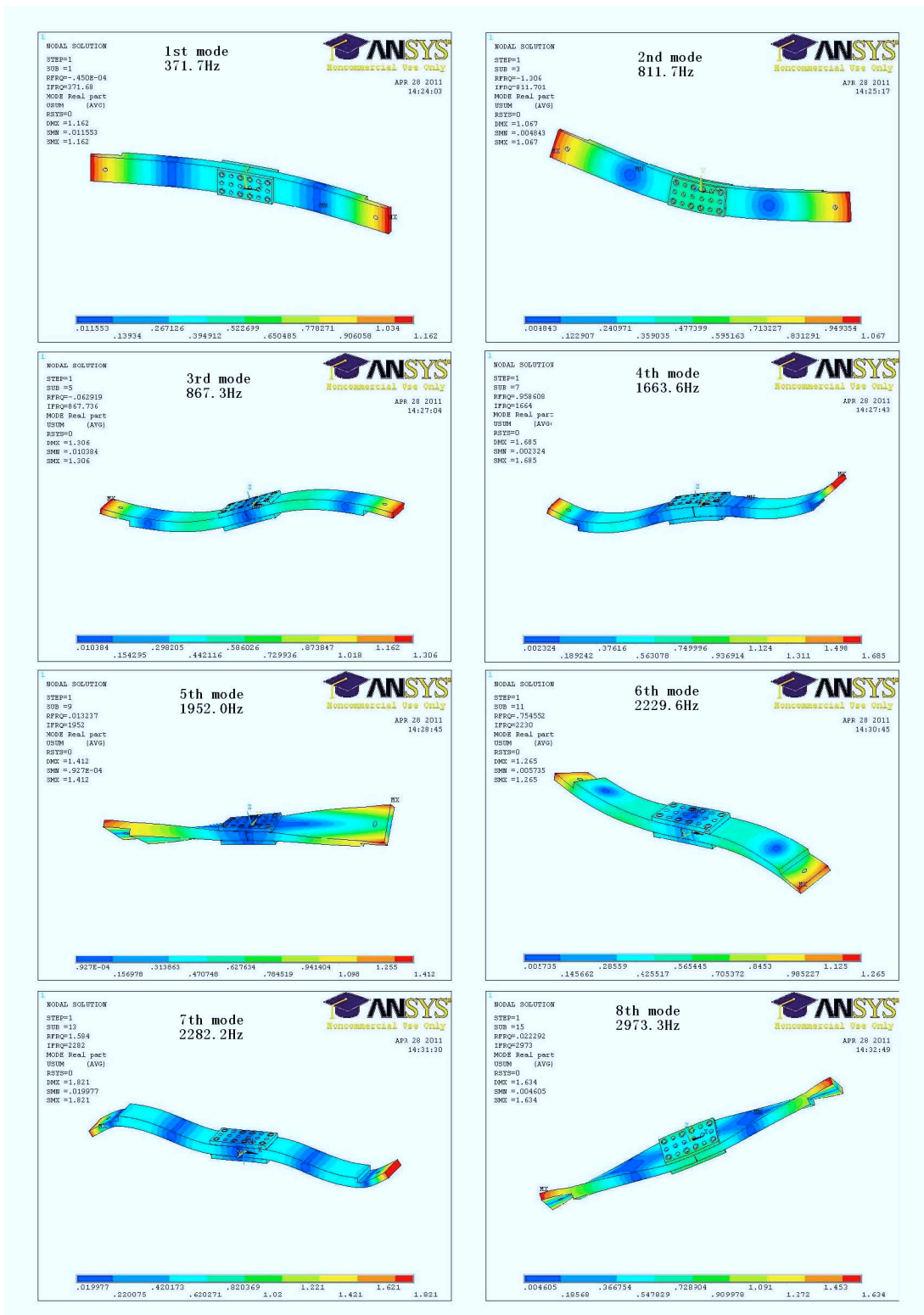


Figure 3.4.: Eigenfrequencies of the assembled Structure



different bolt position for the joint can be applied, which will be discussed in section 5.1.3. This means the structure will provide different types of pressure distributions.

- The structure can perform several different assembly.  
The structures can be assembled in many different ways, with the different joint types. For the thesis, only the structure showed in figure 3.1 will be used.
- The structure is very simple.  
The structure can be nearly considered as several bars connecting to each other with the joints. Each structure can be considered as linear system, and the structures will be satisfy the assumptions for the analytical and experimental modal analysis state in chapter 2.

The structures designed are satisfying the criteria and can be used in the investigation with experimental modal analysis.



## 4. Analytical approach

For the thesis, the X-Modal II which is developed by the Structural Dynamics Research Laboratory of University of Cincinnati (UC-SDRL) will be utilized. This software provides 6 kinds of modal parameter estimation methods. Which method is the more suitable one for the analytical data sets with the low damping will be discussed with the analytical approach in this chapter. The analytical data sets with known properties are generated using the MATLAB code (see appendix A.1). And the analytical data sets will be transferred into Universal File Format (UFF) in order to be loaded into X-Modal II. After calculating the poles and vectors, the poles must be chosen from many possible solutions ( section 4.2.1 ). Two techniques used to select the poles will be compared. The different modal parameter estimation methods will be investigated with respect to several different aspects such as the pole selecting method and the frequency resolution to determine the more suitable method for the data sets with low damping properties.

### 4.1. Analytical Data Sets Creation

First, the Single Input Single Output (SISO) modal model is constructed to generate analytical data sets with different frequency resolutions and these data sets will be used to compare the two methods used to select poles and vectors in X-Modal II. Investigation of the influences caused by different frequency resolutions also requires these data sets. For the frequency domain method, the Multi Input Multi Output (MIMO) modal model used to generate analytical data sets are utilized to determine the better pole selecting method and the frequency resolution for the following investigations.

Second, the MIMO Spatial model with the chosen frequency resolution will be provided. For the modal parameter estimation, the pole selecting method chosen by the first step will be applied. These analytical data sets obtained from the MIMO spatial model will be used to investigate the different modal parameter estimation methods.

At the end, the MIMO modal model with noise is used to generate the analytical data sets to investigate the influence caused by the noise with different amplitude as well as determine which modal parameter estimation method can overcome the uncer-

tainty of the experimental and analytical data sets.

### 4.1.1. Analytical Data Sets With SISO Modal Model

Here the MATLAB code refereced form reference [10] in Appnedix A.1 is used to generate the analytical data sets with the five modes separated in a frequency range of  $0 \sim 1000Hz$ . The data sets with the frequency resolution at  $1Hz$ ,  $0.5Hz$ , and  $0.25Hz$  are given respectively.

**Table 4.1.:** Properties of the SISO modal model data set

Mode	Residue	Damped Natural Frequency (Hz)	Daping Ratio (%)
1	10	128	0.1
2	20	256	0.0833
3	30	512	0.0463
4	39	768	0.0309
5	50.7	806.4	0.0154

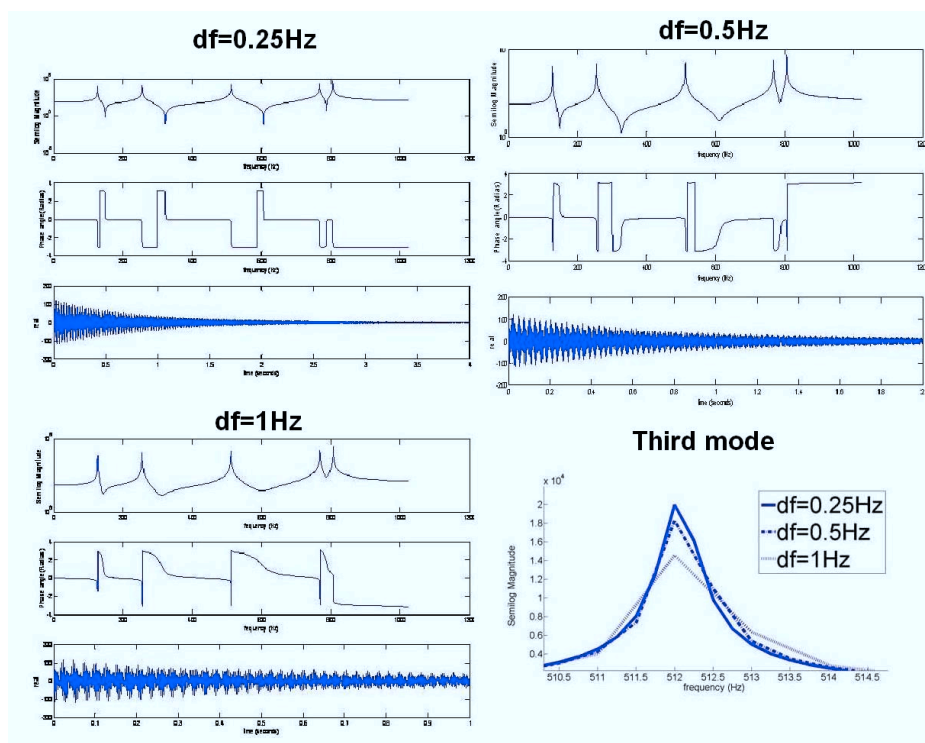


**Figure 4.1.:** Signals of SISO modal model data sets

The plots of Impulse Response Function (IRF), Frequency Response Function (FRF) and Phase angle of analytical data sets with the modal properties showed in table 4.1 at different frequency resolutions are presented in the figure 4.1. At the last of the figure 4.1, the third mode of the FRFs with different frequency resolution have been overlaid. From this, the results that the frequency resolution do not change the eigenfrequency too much, but the damping will be greatly affected for the method use the frequency domain data sets can be derived out.

The data sets created will be transferred into universal file format using the MATLAB code [6]. These data sets are used to determine the suitable frequency resolution for the following analytical models.

#### 4.1.2. Analytical Data Sets With MIMO Modal Model

Here the MIMO modal model will be created with the modal frequencies and mode shapes. The transformation matrix introduced in equation ( 2.25 ) which will used to create the MIMO system can be constructed with the mode shapes as columns. The modal damping properties and damped natural frequencies of this model are the same as the table 4.1. Here the transformation matrix of the original system will be given as equation ( 4.1 ).

$$\psi = \begin{bmatrix} -10 & -10 & -10 & -10 & -10 \\ 5 & 10 & 5 & 5 & -5 \\ 10 & 0 & -15 & 0 & 10 \\ 5 & -10 & 5 & -5 & -5 \\ -10 & 10 & -10 & 10 & -10 \end{bmatrix} \quad (4.1)$$

The frequency resolution is 1Hz which will be determined in the section 4.2.2. These data sets are used to find out what kind of influences will be caused by the different noise amplitudes.

#### 4.1.3. Analytical Data Sets With MIMO Spatial Model

The spatial model is developed from the structure showed in figure 2.2. The degree of freedom (DOF) for this system is five. The system contains five mass points, four damping and four stiffness which are between each mass as well as two damping and two stiffness which are between the first and last mass and the environments. The mass, damping and stiffness will be provided in table 4.2 for the spatial model.

Here the first five modes lie in the frequency range of 0 to 1000Hz. The analytical data sets with MIMO spatial model are generated with the above physical parameters such as mass, stiffness and damping, and the modal properties can be calculated out

**Table 4.2.:** The Values of Mass, Stiffness and Damping

Mass(Kg)		Stiffness(N/m)		Damping(Kg/s)	
m1	30	k1	9E+07	c1	60
m2	20	k2	15E+07	c2	70
m3	25	k3	15E+07	c3	80
m4	20	k4	15E+07	c4	90
m5	25	k5	20E+07	c5	100
		k6	10E+07	c6	110

and summarized in table 4.3. In order to get the MIMO data sets, the sensors are supposed to be located on the second and fifth mass, and the impact hammer is used to hit at each mass point. This means the output or response indexes are 2 and 5; the input or reference indexes will be from 1 to 5. This is just similar to the process of the experimental modal analysis in which the sensor (response) will be fixed and the actuator (input) is moved. As a consequence, 10 data sets for the frequency resolution given are created. These data sets are used to compare the different modal parameter estimation methods and to determine the more suitable method for the data process with the data sets acquired from the experiment.

**Table 4.3.:** Properties of the MIMO spatial model data set

Frequency (Hz)	Damping ratio (%)
181.2	0.0457
351.1	0.0781
517.3	0.0974
724.4	0.1177
827.9	0.1442

## 4.2. Investigation of Modal Parameter Estimation Methods

After creating the analytical data sets, these data sets will be transferred into universal file formats using the MATLAB code, then the UFF file will be loaded into X-Modal II to perform the modal parameter estimation with several different methods. The modal

parameters can be obtained in terms of eigenfrequencies (damped natural frequencies) and modal damping ratio. The exact eigenfrequencies and the damping ratio are already known in the section 4.1, and the methods will be investigated by the comparison of the exact value and the values acquired from the X-Modal II. This detail procedure can be found in the reference [24]. The user interface of modal parameter estimation of the X-Modal II showed in figure 4.2.

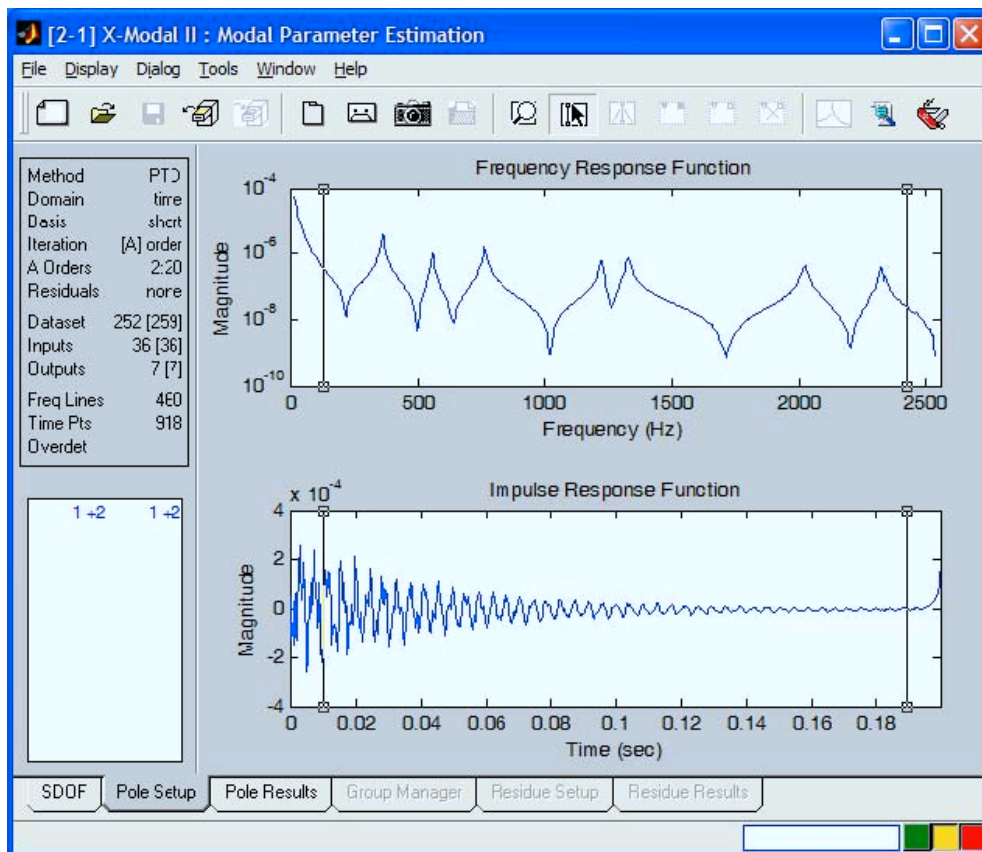
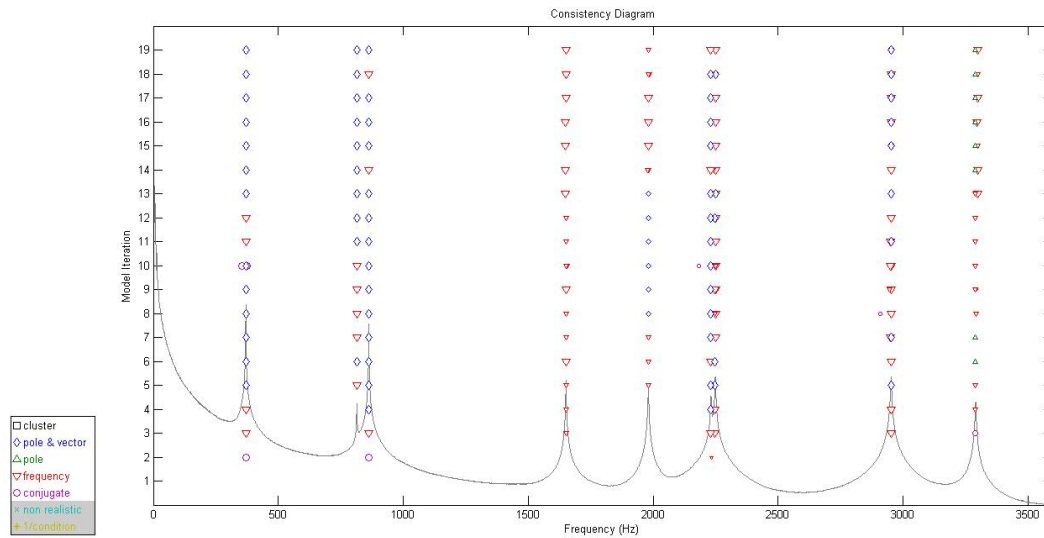


Figure 4.2.: MPE user interface of X modal II [17]

### 4.2.1. Pole Selecting Methods

First, the methods used to select the poles and vectors with X-Modal II must be determined with the help of the consistency diagram (figure 4.3) or density diagram (figure 4.4). Consistency diagram is one of the most common methods for determining the proper poles and vectors. It is developed by computing different modal solutions with respect to model orders, normalization methods and equation condensation methods. Different model solutions are shown in this diagram and it is hard to select the proper solutions among such a mess. Generally, pole surface density diagrams are more pow-

erful than consistency or stability diagrams at locating similar pole vector estimates from all of the possible solutions represented in the consistency diagram [18]. The high density of the pole surface density plot means there are a large number of solutions for the modal parameters [2] and the poles of this region are supposed as the proper solutions. The detail can be found in reference [18], reference [5] and reference [2]



**Figure 4.3.:** Consistency Diagram for Experiment Datasets

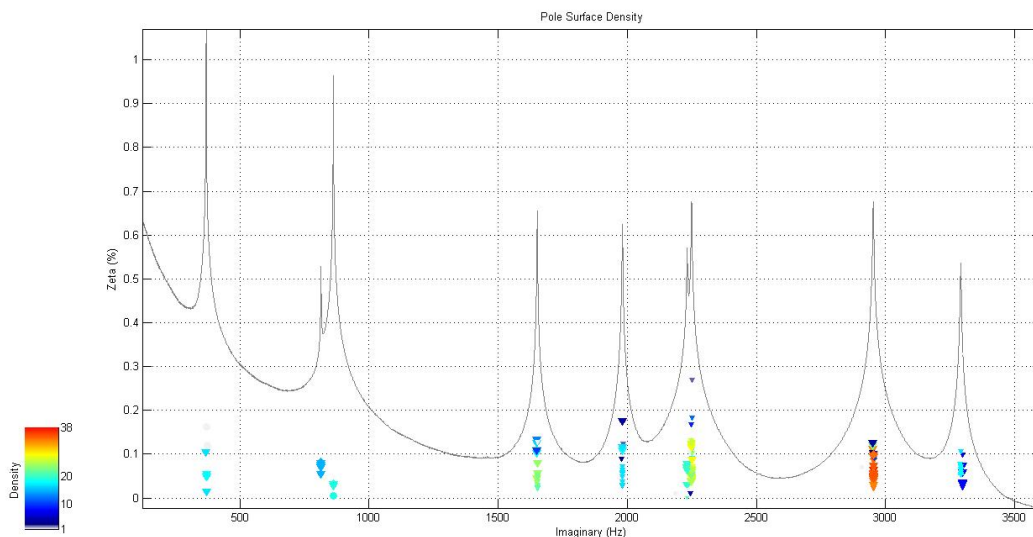


**Figure 4.4.:** Pole Surface Density Diagram for Experiment Datasets

Zoom in the high density region in the density diagram (figure 4.5), there are also many possibilities of poles and vectors. In order to select one pole, there are two kinds



of methods provided. First method is to select a pole near the centroid of the poles with high density and this is indicated as method A; second method is to create a pole at centroid of the poles with high density indicating method B. How to select the region is also a problem. Generally, rectangles which can contains the consist poles as many as possible and do not contains bad estimations at the same time (figure 4.5) will be used to select the region. For these two methods, it will perform several times and take the average as the final results of modal parameters.

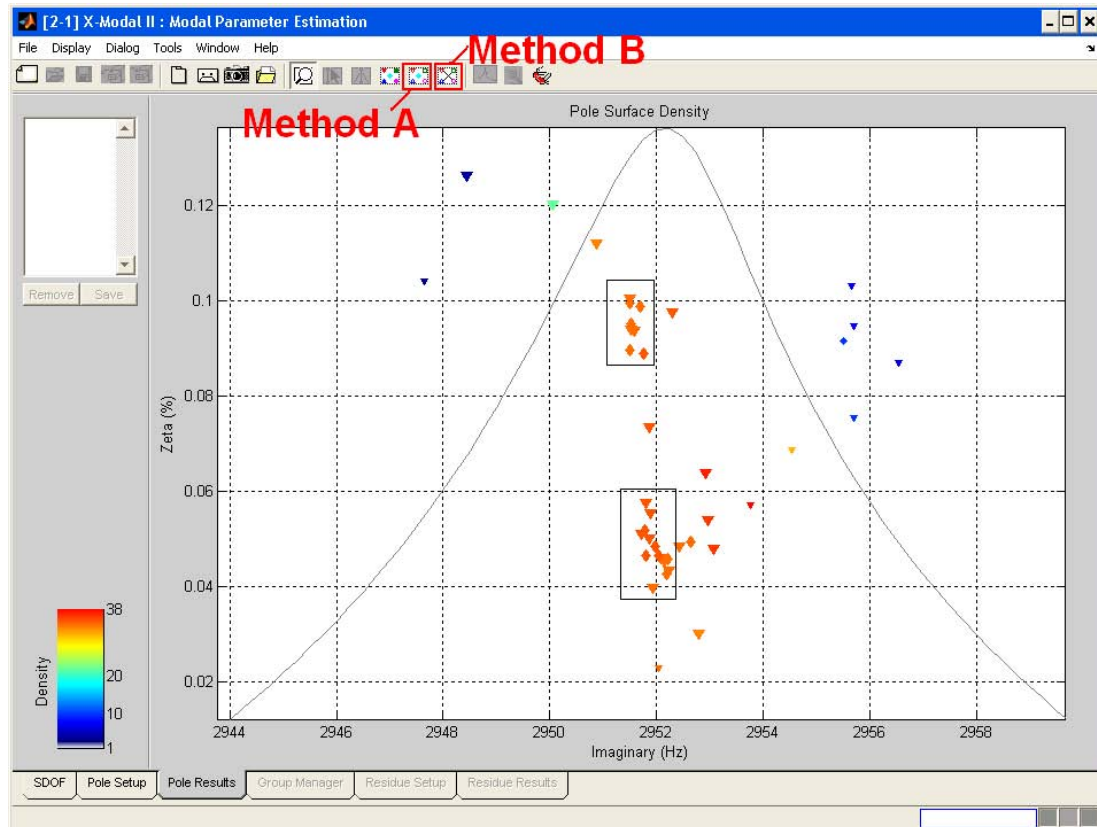


**Figure 4.5.:** Pole Selectiong Mehods with X-Modal II

Which method give better estimation of modal parameters with different frequency resolutions is the priority. For this investigation following parameters are selected.

- Model: SISO modal model
- MPE Method: PTD, RFP, RFP-Z (as ERA and PFD is MIMO method)
- Frequency Resolution: 1Hz, 0.5Hz, 0.25Hz
- The exact modal parameters provided in tabel 4.4

**Table 4.4.:** The Exact Properties for SISO Modal Model

Mode Nr.	1	2	3	4	5
Freq(Hz)	128	256	512	768	806.4
Damping(%)	0.1000	0.0833	0.0463	0.0309	0.0154

For this investigation, analytical data sets for each frequency resolution are created. The modal parameter estimation is carried out for these data sets with different pole selecting methods. From the MPE results of modal parameters, summarization was made to make the things easy to understand. Pole selecting methods at the same frequency resolution for different modal parameter estimation methods are investigated with the average errors for frequency and damping respectively in table 4.5, table 4.6 and table 4.7.

**Table 4.5.:** The Average Error with SISO Modal Model at Frequency Resolution 1Hz

Method	Error(%)	A	B
PTD	Freq	0.0497	0.0496
	Damp	0.7513	0.4993
RFP	Freq	0.0451	0.0407
	Damp	11.9600	15.2600
RFP-Z	Freq	0.0486	0.0246
	Damp	0.1279	0.0000

**Table 4.6.:** The Average Error with SISO Modal Model at Frequency Resolution 0.5Hz

Method	Error(%)	A	B
PTD	Freq	0.0246	0.0247
	Damp	0.6353	0.5361
RFP	Freq	0.022	0.0184
	Damp	11.2100	10.9100
RFP-Z	Freq	0.0246	0.0246
	Damp	0.5704	0.6382

**Table 4.7.:** The Average Error with SISO Modal Model at Frequency Resolution 0.25Hz

Method	Error(%)	A	B
PTD	Freq	0.0112	0.0115
	Damp	0.7749	0.5588
RFP	Freq	0.0109	0.0099
	Damp	12.3900	5.9400
RFP-Z	Freq	0.012	0.0121
	Damp	1.1300	1.1700

From table 4.5, table 4.6 and table 4.7, conclusions can be made that the eigenfrequencies will not differ too much with respect to pole selecting methods. For all the modal parameter estimation methods used and for all the frequency resolutions given, the method B, which creates a pole at centroid, gives better estimation of the damping ratio. The method B will provide better estimation since it averages the poles inside the rectangle and has the informations about the system. While the method A will only select one pole near the center of region of square and the results only related to the rectangle used to select the poles. This will have less information of the system.

#### 4.2.2. Frequency Resolution

From the results above, the effect caused by the frequency resolution with respect to PTD, RFP and RFP-Z methods can be noticed. The results are written in another way so that it is easy to understand. For the investigation, the following results will be used.

- Pole selecting method B

**Table 4.8.:** The Average Error with SISO Modal for Different Frequency Resolutions

Average error (%)						
Method	PTD		RFP		RFP-Z	
Df	Freq	Damp	Freq	Damp	Freq	Damp
1Hz	0.0496	0.4993	0.0407	15.2600	0.0246	0.0000
0.5Hz	0.0247	0.5361	0.0184	10.9100	0.0246	0.6382
0.25Hz	0.0115	0.5588	0.0099	5.9400	0.0121	1.1700

From the table 4.8, the conclusion can be made that for time domain or z-domain method, the frequency resolution will not play too much role for results of modal parameters. Because the time domain method and z-domain method do not use the frequency domain information. For the frequency domain methods, the average error will get smaller as the frequency resolution get finer, which means the damping will be more accurate as the frequency resolution get smaller.

Here the investigation of what kind of role the frequency resolution plays in frequency domain methods is carried out. For this investigation, following parameters are selected.

- Model: MIMO modal model
- MPE Method: RFP and PFD
- Frequency Resolution:  $1Hz$ ,  $2Hz$ ,  $3Hz$
- Pole selecting method: Method B
- The exact modal properties in the table 4.9

**Table 4.9.:** The Exact Properties for MIMO Modal Model

Mode Nr.	1	2	3	4	5
Freq(Hz)	127.9999	255.9999	512.0000	768.0000	806.4000
Damp(%)	0.1000	0.0833	0.0463	0.0309	0.0154

The frequency resolution will not change the eigenfrequency too much, but it will affect the damping a lot with frequency domain methods. The frequency resolution can be considered as the sampling frequency. As the sampling frequency get bigger, the analytical data sets in the form of Frequency Responce Function start to lose some informations (figure 4.1). The frequency domain methods will use data sets in the form of FRF to perform the modal parameter estimation. so the damping will be overestimated.

From the result in the table 4.10, the relation can be noticed that as the frequency resolution getting bigger, the average error for eigenfrequencies and damping get bigger when using the frequency domain MPE methods. This is satisfy the theoretic analysis and reasonable.

Conclusions can be made from the table 4.8 and table 4.10 that, the estimation of modal parameters using time domain method is much better than frequency domain methods. For the analytical analysis, the frequency resolution will be set to  $1Hz$ .

**Table 4.10.:** The Average Error with MIMO Modal Model for Different Frequency Resolutions

Average error (%)				
Method	RFP		PFD	
Df	Freq	Damp	Freq	Damp
1Hz	0.0467	3.029	0.0477	5.406
2Hz	0.0943	18.823	0.0955	4.954
3Hz	0.2106	38.484	0.2274	16.413

### 4.2.3. Modal Parameter Estimation Methods

The method for selecting the poles with X-Modal II has been determined in the previous section. The frequency resolution is set to  $1Hz$ . Which method shows better modal parameter estimation for analytical data sets with low damping need to be investigated. For this task, the following parameters will be utilized.

- Model: MIMO modal model
- MPE Method: PTD, ERA, RFP, PFD, RFP-Z
- Frequency Resolution:  $1Hz$
- Pole selecting method: Method B
- Exact modal properties given in table 4.11

**Table 4.11.:** The Exact Properties for MIMO Spatial Model

Mode Nr.	1	2	3	4	5
Freq(Hz)	181.206	351.0845	517.2696	724.3909	827.8862
Damping(%)	0.0457	0.0782	0.0974	0.1177	0.1442

From the MPE results with MIMO spatial model, summarization is made in the table 4.12 to make the things easy to understand.

It can be seen from the table 4.12 that, five MPE methods all gives good estimation for the eigenfrequencies. However, the PTD method gives best estimation for damping followed by PRF-z method. the next are RFP method and PFD method. ERA method gives the worst estimation of damping as the data sets has few spatial informations.

**Table 4.12.:** The Average Error with MIMO Spatial Model(1Hz and Method B)

Average error (%)					
Method	PTD	ERA	RFP	PFD	RFP-Z
Freq	0.0007	0.0025	0.0079	0.0012	0.0016
damp	0.3657	4.2452	2.3298	2.6343	1.1269

Then the investigation of modal estimation method with respect to random noise is carried out with the data sets generated from MIMO spatial model added with noise. Here, which method shows better resistance against the noise will be checked out, and for this investigation the following parameters will be utilized.

- Model: MIMO modal model with noise
- MPE Method: PTD, ERA, RFP, PFD, RFP-Z
- Frequency Resolution:  $1Hz$
- Pole selecting method: Method B
- Exact modal properties in table 4.9.
- The amplitude of the random noise: 0 001

The MPE results will be summarized in table 4.13.

**Table 4.13.:** The Average Error with MIMO Modal Model with Random Noise

Average error (%)					
Method	PTD	ERA	RFP	PFD	RFP-Z
Freq	0.0488	0.0476	0.043	0.0319	0.0491
damp	1.0559	3.6864	3.6827	10.5711	1.9486

The same result as the previous investigation can be derived from the table 4.13 with a little difference. The error for eigenfrequencies and damping are all become bigger than the case without noise. PTD method still gives the best estimation for damping. Investigation for PTD method with respect to the amplitude of noise will be carried out and the MPE results are summarized in the table 4.14.

**Table 4.14.:** The Average Error with MIMO Modal Model with Different Noise Amplitude

Average error (%)			
Noise amp	0.001	0.005	0.01
Freq	0.0491	0.0494	0.0500
Damp	1.0188	3.6693	4.3443

It can be seen from the table 4.14 that, as the amplitude of the noise getting bigger, the average error for damping will get bigger since the noise means more energy dissipation.

It can be concluded from the investigations in this chapter that, when using the same data sets, the PTD gives best estimation, followed by PRF-Z. PFD method gives worst estimation. For our data sets, time domain methods gives better estimation than frequency domain method. For the data processing with experimental data sets, PTD method will be applied.

Time domain methods tend to provide the best results when a large frequency range or large numbers of modes exist in the data. The frequency domain models tends to provide the best results when the frequency range of interest is limited and the number of the modes is relatively small [15].

High order methods require more spatial data because they use only a limited subset of spatial data (i.e. fewer physical DOFs); therefore, they work well when many time or frequency data points are measured. Low order models must be used when measurements at many points are made at only few time points [1].

As the frequency range of the system is  $0 \sim 3000Hz$ , the PTD which is high order time domain method will obtain better results than the other methods. For ERA, this method is not suitable for our system since the data has a few input and output points (spatial information). Also the system creates the IRF and then transferred the data into FRF using FFT. With the usage of FFT, the information of the original system will get lost. As a result, the frequency domain method shows bad results. The z domain method is very stable and shows good performance. But the error is still bigger than PTD. The PTD method will be chosen for processing the experimental data sets.





# 5. Experiment and Simulation

After structures designed and manufactured, the experiment is carried out in order to get the impulse response function or frequency response function used to perform modal parameter estimation. First, each part of the total structure separately is tested in order to adjust the material parameters such as density, Young's modulus and Poisson's ratio. The structures are assembled and suspended with elastic ropes. then free-free boundary condition experiment are performed by hitting the structure with impact hammer. The several sets of frequency response function are obtained from the experiment. The data sets are stored in the form of universal file format and loaded into X-Modal II directly. The PTD method is applied to do the modal parameter estimation so as to get the dynamic properties. The process is repeated with the assembly with different joint properties such as different torques and different bolt positions. Then the commercial software ANSYS is used to doing the structure analysis including modal analysis and harmonic analysis. The modal analysis is used to verify the relationship between the joint characteristics such as normal force in the joint and the the pressure distribution of the joint and the modal parameters especially eigenfrequencies; the harmonic analysis is used to get the frequency response function of the structure, the data will transfer into universal file format and loaded into X-Modal II to calculate the modal parameters, here the interrelation between the joint characteristics mentioned above and damping properties. The thin layer methods will be applied.

## 5.1. Experiment

The purpose of the experiment is to get the FRF data sets with impact hammer and accelerometers. The separate parts of our structure are showed in figure 5.1 and the two pieces of part B and two pieces of part C are used to construct the total system.

### 5.1.1. Experimental System Description

The experiment setup is showed in figure 5.2. The structure will be discretized and the nodes are defined as figure 5.3. the structured is suspended freely and attached with

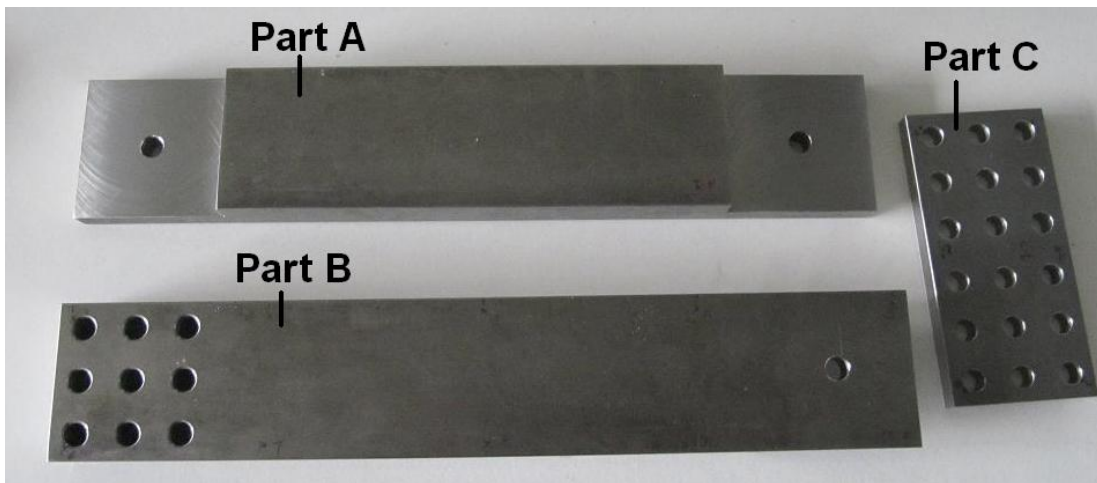


Figure 5.1.: Part A, Part B and Part C

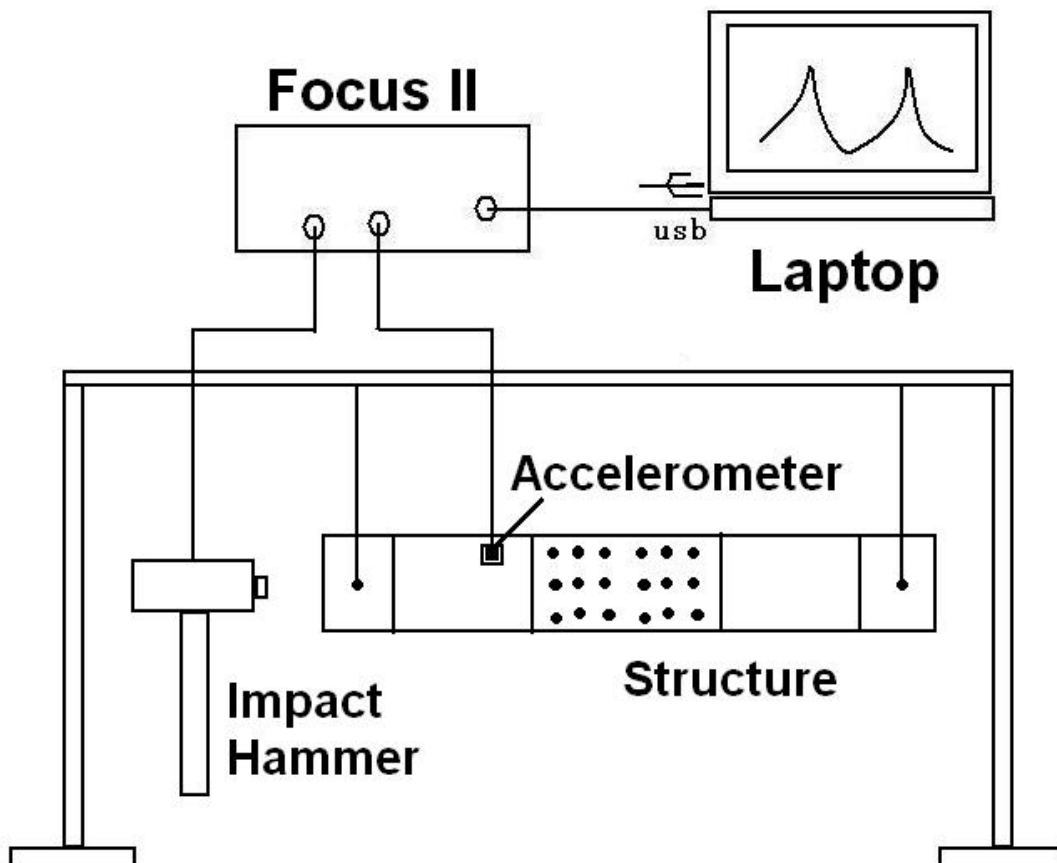
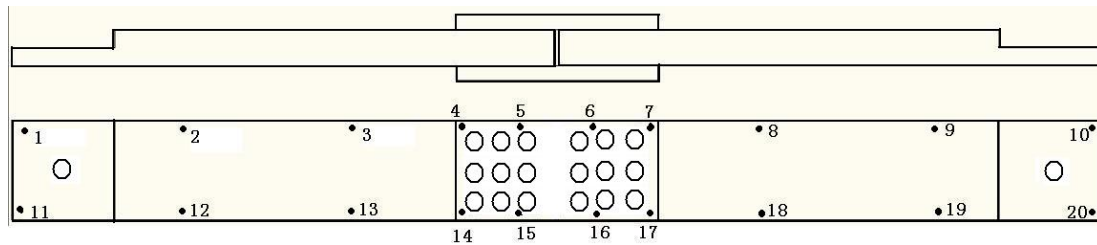


Figure 5.2.: Experiment Setup

accelerometers. The accelerometer must attach to the nodes which can be excited in most modes. Attaching the accelerometer to the zero nodes for some modes need to be avoided. The cables of accelerometers and impact hammer must connect to the signal processing device named Focus II and the Focus II will be connected to the laptop with the USB connection. Then the impact hammer experiment is carried out.



**Figure 5.3.:** Discretization of the Measured Structure

Some points must be paid attention to. First, the structure need to be suspended with flexible rope so that the resonance frequencies of these ropes to the system are far away from the frequency range of interest. Second, the right tip of the impact hammer must be selected. Different tips excite different frequency range. According to the frequency range of interest, the proper tip must be selected. Third, the structure must hit with impact force at  $150 \pm 25N$  since the impact force affects dynamic properties especially the damping ratio [23]. At last double hitting must also be avoided in order to get the Impulse Responce Function.

Two pieces of part A, four pieces of part B and two pieces of part C are manufactured and marked with A-1, A-2, B-1, B-2, B-3, B-4, C-1, C-2, C-3, C-4. The mass of these part showed in in table 5.1.

**Table 5.1.:** Mass of Each Part of Real Structure

Part	Mass (kg)	Part	Mass (kg)
A-1	2.0790	A-2	2.0792
B-1	2.2534	C-1	0.3235
B-2	2.2451	C-2	0.3245
B-3	2.2476	C-3	0.3252
B-4	2.2518	C-4	0.3239

For the mechanical system, B-1, B-4 and C-1, C-4 are selected to assemble the system since the mass of this parts is closed to each other. Here the mass of the bolts

also need to be taken into consideration as the mass attaching to the structure affect the damping and eigenfrequencies as showed in figure 5.4.

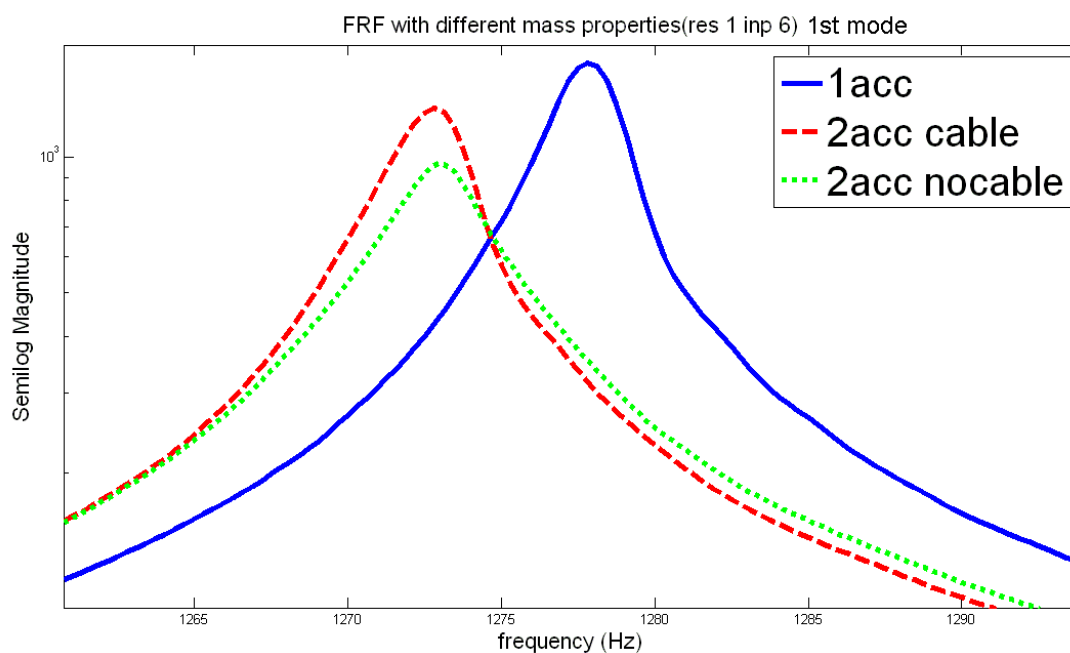


**Figure 5.4.:** Massloading Effect for Part A at 1st Mode

Here a very simple investigation about the massloading effect is carried out. The part A is used and attached with the accelerometer at nodes 1 and 3, then hit the nodes 6 and get the FRF data. The results can be seen from table 5.2 and table 5.3. When

**Table 5.2.:** Effect of Mass attached and cable for Input -6z Output 1z

I-6z O1z	Mode Nr.	1	2	3	4
With 1acc	Freq(Hz)	1277.7	2431.2	3525.9	4099.1
	Damping(%)	0.0932	0.1638	0.3974	0.2986
With 2acc Withcable	Freq(Hz)	1272.5	2421.8	3501.6	4007.9
	Damping(%)	0.1062	0.5574	0.3823	0.2514
With 2acc No cable	Freq(Hz)	1272.7	2432	3500.6	4006.2
	Damping(%)	0.1548	0.5272	0.2837	0.3225

additional mass is added to the structure, the eigenfrequencies for each mode tend to become smaller. However the error for eigenfrequencies stays in 0.6% whereas error for damping of certain modes is exceed 100%. When the mass is attached to

**Table 5.3.:** Effect of Mass attached and cable for Input -6z Output 3z

I-6z O3z	Mode Nr.	1	2	3	4
With 1acc	Freq(Hz)	1286.4	2461.2	3554.5	4013.9
	Damping(%)	0.0237	0.0379	0.0141	0.0266
With 2acc Withcable	Freq(Hz)	1285.3	2461.4	3554.2	4010.9
	Damping(%)	0.0608	0.0416	0.0237	0.0418
With 2acc No cable	Freq(Hz)	1285.6	2461.3	3553.8	4011.2
	Damping(%)	0.0585	0.0247	0.014	0.0398

the low mass part (which has big deformation), the effect is much bigger. So the accelerometers are better to attached to the part has bigger mass.

### 5.1.2. Experimental Procedure

In order to adjust the material parameters for our structure, the experimental modal analysis will be carried out for each part of the structure. All the structures are need to be descretize and the nodes must be marked on the structures. After connecting all the cables and equipments, the flexible ropes are used to suspend the structure to the supporting frame and the accelerometers are attached to the structures. Each node are hit by the impact hammer and the frequency response functions are obtained from the signals of accelerometers processed by the Focus II into the computer. The data sets are stored in universal file format. The impact hammer experiment is showed in figure 5.5.

The nodes for part A, part B and part C is showed in figure 5.6. For part A, the accelerometer is attached at the node 1 and 9, then all nodes are hit to get the frequency response functions. For part B, the accelerometer is attached at node 2 and 10, all the nodes are hit to get the FRF. For part C, the accelerometer is attached at node 6 and 2, then all the nodes are hit to get the FRF. Note that, here only one accelerometer is used to avoid the massloading effect. The data sets obtained will be used to adjust the material parameters of the system, especially density and Young's modulus.

Then the experimental modal analysis with the assembled structure is carrid out. Here the effects of different torques used to fastening the bolts and different position and numbers of bolts will be taken into consideration. Four kinds of bolt positions named Type A, Type B, Type C and Type D are showed in figure 5.7. The real system with the bolt position type D is showed in figure 5.8. The torques used for fastening

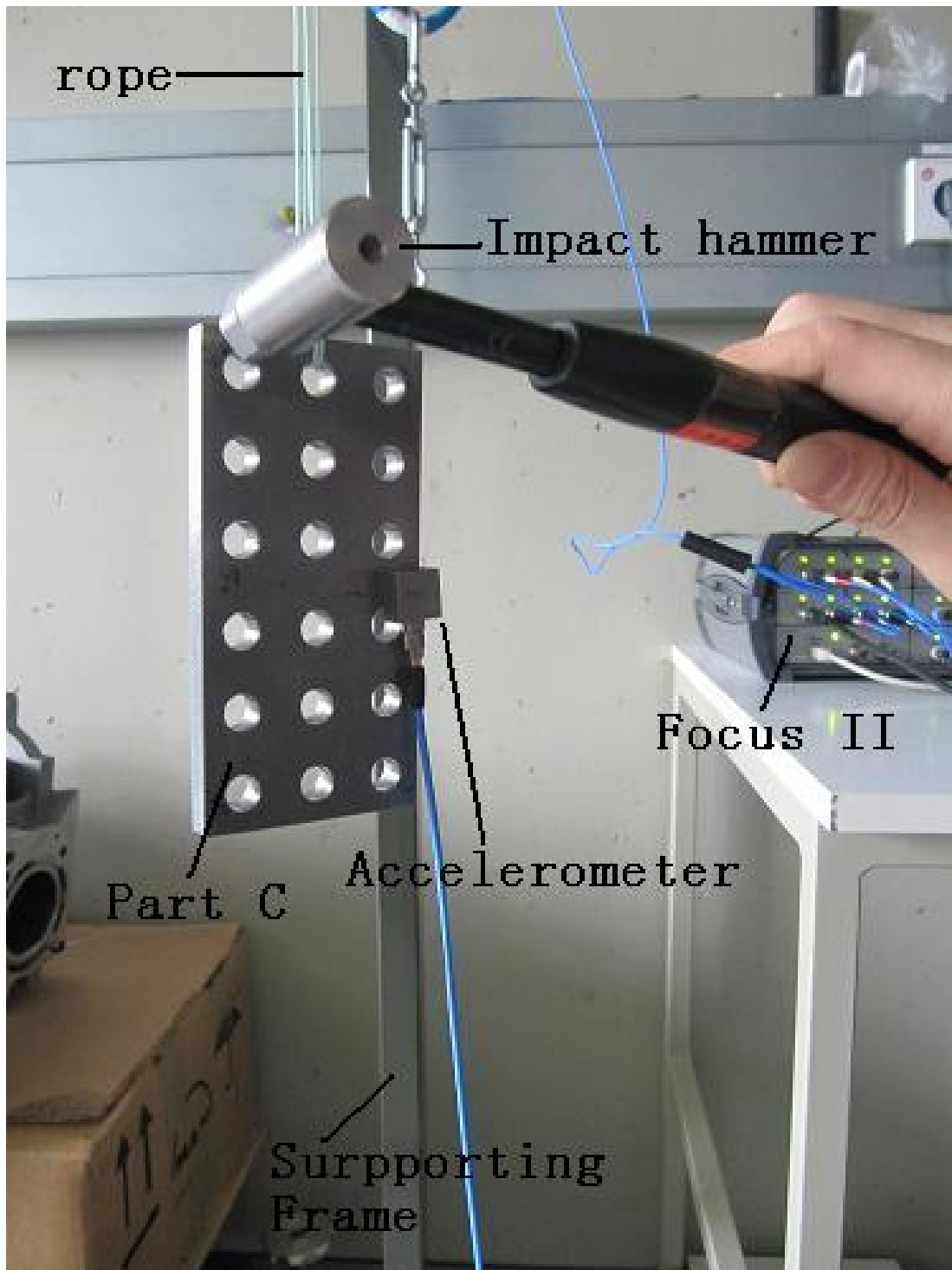
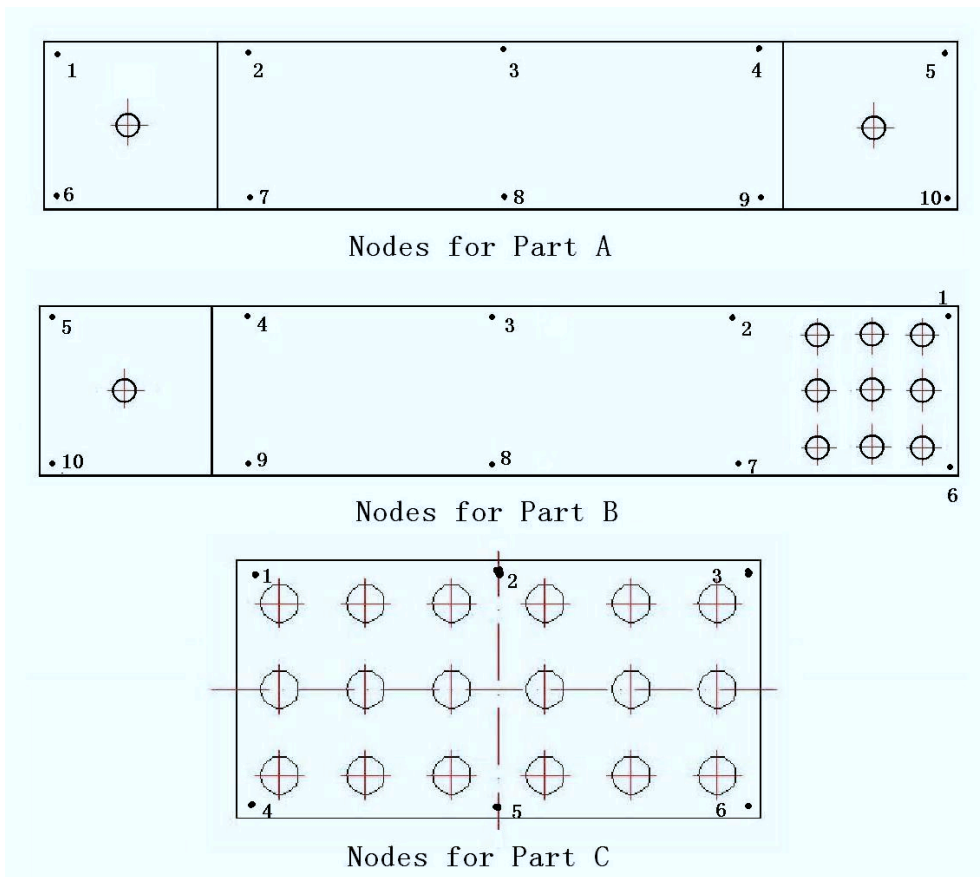
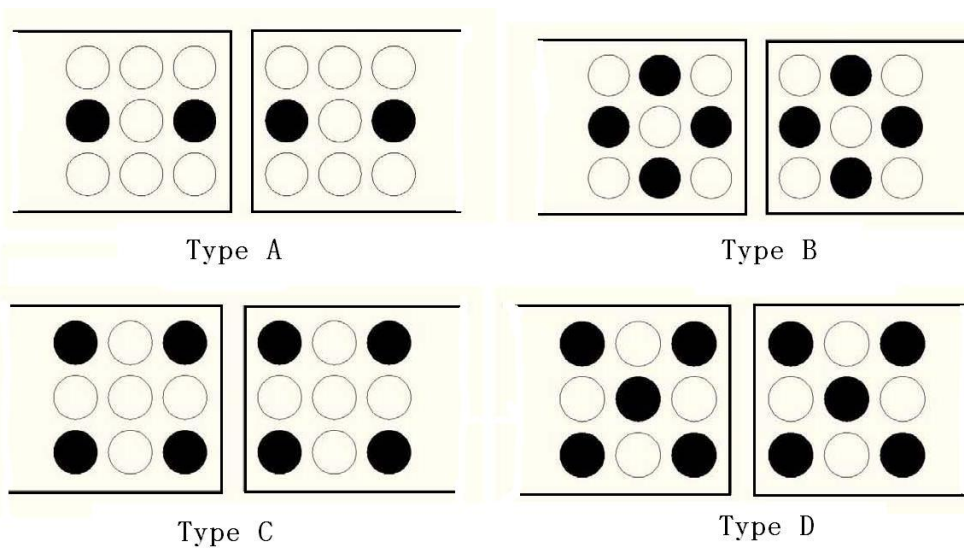


Figure 5.5.: Impact Hammer Experiment for Part C



**Figure 5.6.:** Nodes for the part A, part B and part C



**Figure 5.7.:** Types of Different Positions of Bolts



**Figure 5.8.:** Real System of Bolt Position Type D

the bolts are  $10Nm$ ,  $20Nm$  and  $30Nm$ . For Type A, the impact hammer experiment with the torques  $10Nm$ ,  $20Nm$  and  $30Nm$  will be performed. For Type B, torques of  $20Nm$  and  $30Nm$  are applied for the experiment. For Type C, torques of  $20Nm$ ,  $30Nm$  are used. For Type D, torque of  $30Nm$  is used. The experiments performed are showed in the table 5.4.

**Table 5.4.:** The Experiments performed

Torque(Nm)	10	20	30
Type A	•	•	•
Type B		•	•
Type C		•	•
Type D			•

During the experiments, the total structure are constructed and the nodes for assembled system showed in figure 5.9. The accelerometers are attached at the nodes 4 and 8, and then nodes from 1 to 20 are hit to get the FRF of the assembled structure.



**Figure 5.9.:** The Total System with Bolt Position Type A

The FRFs get from the experiments will be processed by the X-Modal II and used



to investigate the influence of the joints characteristics on the modal parameters.

### 5.1.3. Data Processing

In this section, data processing is performed. The data sets get from the impact hammer experiments are loaded into X-Modal II and the modal parameter estimation is carried out.

**First**, the data sets from the experiment with each part of the system are dealt with. For part A, part B and part C, the modal parameters can be calculated from X-Modal II and showed in table 5.5. This table will be used to adjust the material parameters of the system including density, Poisson's ratio and Young's modulus in section 5.2.1. The damping for Part C is much bigger than Part A and Part B since the mass effect is bigger in the structure with low mass.

**Table 5.5.:** Modal Parameters for Part A, Part B and Part C

	Mode Nr	1	2	3	4	5
Part A	Freq(Hz)	1287.4	2459.1	3474.5	3549.3	4013.9
	Dmp(%)	0.0085	0.0311	0.0290	0.0187	0.0249
Part B	Freq(Hz)	1255.4	2719.8	3230.0	3483.0	
	Dmp(%)	0.0050	0.0572	0.0177	0.0162	
Part C	Freq(Hz)	3017.5	3701.7			
	Dmp(%)	0.3735	0.2089			

**Then**, the Modal Parameter Estimation (MPE) is carried out using the data sets obtained from the experiment with the total system with different bolt position types and different fastening torques. In the modal parameter estimation for the assembled structure, the MPE is performed for three times and the average of the three results will be used as the final result. The results are summarized in the way that the relationship between dynamic properties and different joint characteristics can be easily seen from.

The results with respect to the torque for each bolt position type are summarized. The table 5.6 shows the modal parameters for type A at the torque with 10Nm, 20Nm and 30Nm. The table 5.7 shows the modal parameters for type B at the torque with 20Nm and 30Nm. The table 5.8 shows the modal results for type C at the torque with 20Nm and 30Nm. Then the relation of modal properties and the torque used to fastening the bolts which related to the normal force at the joints is investigated.

**Table 5.6.:** Modal Parameters for Type A with Torque 10Nm, 20Nm and 30Nm

Mode \ T (Nm)	Freq(Hz)			Dmp(%)		
	10	20	30	10	20	30
1	364.8	368.7	369.7	0.0456	0.0421	0.0419
2	722.3	739.4	743.9	0.1489	0.0959	0.0977
3	861.9	864.8	865.5	0.0323	0.0209	0.0307
4	1629.9	1642.7	1646.7	0.121	0.1044	0.0608
5	1791.5	1844.9	1857.7	0.237	0.2141	0.1724
6	2192.6	2203.2	2205.3	0.1092	0.0718	0.1747
7	2241.6	2254.8	2258.4	0.1163	0.0877	0.0605
8	3018.6	3022.4	3033.1	0.2028	0.1716	0.1232

**Table 5.7.:** Modal Parameters for Type B with Torque 20Nm and 30Nm

Mode \ T (Nm)	Freq(Hz)		Dmp(%)	
	20	30	20	30
1	365.2	367.8	0.0434	0.044
2	768.6	772.6	0.0824	0.0747
3	861.4	863	0.0406	0.0353
4	1636.5	1643	0.0747	0.0631
5	1921.9	1933.2	0.1292	0.086
6	2212.2	2215.3	0.0829	0.0753
7	2241.5	2248.6	0.1125	0.0482
8	2963.5	2966.2	0.3055	0.1457

**Table 5.8.:** Modal Parameters for Type C with Torque 20Nm and 30Nm

Mode \ T(Nm)	Freq(Hz)		Dmp(%)	
	20	30	20	30
1	368.6	370.5	0.0466	0.0533
2	812.3	818.7	0.1107	0.0704
3	862.1	863.5	0.0696	0.0287
4	1646.1	1652.2	0.0667	0.0588
5	1965	1975.4	0.0834	0.0683
6	2229.1	2233.3	0.0661	0.0523
7	2247.5	2252.5	0.0627	0.0622
8	2960.8	2966.2	0.0695	0.0548

From the results above, conclusions are made about the influence of the torque used to fasten the bolts which is related to the normal force at the joints.

- For the same bolt position type, the eigenfrequencies for each mode get bigger as the torque getting bigger. It can be seen from this result that, the structure gets stiffer as the torque getting bigger. As the normal force at the joint getting bigger, the displacement at the joints gets smaller, and the deformation at the joint also gets smaller. This means that when modeling the joint, big Young's modulus must be given to the joint model at the point where the bolt is applied. The Young's modulus for the joints model gets bigger as the torque or the normal force at the joint getting bigger.
- For the bolt position type A, there is no specific rules for damping with respect to torque. But for the bolt position type B and type C, the modal damping ratio tends to get smaller as the torque getting bigger since the damping in the structure is depending on the deformation in the joint occurring due to a certain mode shape [23]. The pressure distribution happens near the vicinity of the bolts. For Type A, there are only two bolts for the joint and the pressure distribution for the part without bolts will not change linearly during the changes of torque. The effects of non-linearity occurred, as a results the damping has no specific pattern. For Type B and Type C, the deformation of the structure gets smaller as the normal force getting bigger which means the damping ratio also gets smaller as the torque getting bigger.

**At last**, the results with respect to the bolt position type for different torque are

concluded. Table 5.9 shows the modal parameters using the torque  $30Nm$  for the bolt position type A, type B, type C and type D. Table 5.10 shows the modal parameters using the torque  $20Nm$  for type A, type B and type C. Then the relation between the different bolt position type and joint modal parameters are investigated.

**Table 5.9.:** Modal Parameters for Torque  $30Nm$  with Type A,B,C,D

Mode \Type	Freq(Hz)				Dmp(%)			
	A	B	C	D	A	B	C	D
1	369.7	367.8	370.5	370	0.0419	0.044	0.0533	0.0455
2	743.9	772.6	818.7	814.4	0.0977	0.0747	0.0704	0.0582
3	865.5	863	863.5	862.3	0.0307	0.0353	0.0287	0.0268
4	1646.7	1643	1652.2	1651.7	0.0608	0.0631	0.0588	0.0423
5	1857.7	1933.2	1975.4	1981.3	0.1724	0.086	0.0683	0.0554
6	2205.3	2215.3	2233.3	2231.7	0.1747	0.0753	0.0523	0.0560
7	2258.4	2248.6	2252.5	2248.9	0.0605	0.0482	0.0622	0.0672
8	3033.1	2966.2	2966.2	2952.3	0.1232	0.1457	0.0548	0.0477

**Table 5.10.:** Modal Parameters for Torque  $20Nm$  with Type A,B,C

Mode \Type	Freq(Hz)			Dmp(%)		
	A	B	C	A	B	C
1	368.7	365.2	368.6	0.0421	0.0434	0.0466
2	739.4	768.6	812.3	0.0959	0.0824	0.1107
3	864.8	861.4	862.1	0.0209	0.0406	0.0696
4	1642.7	1636.5	1646.1	0.1044	0.0747	0.0667
5	1844.9	1921.9	1965	0.2141	0.1292	0.0834
6	2203.2	2212.2	2229.1	0.0718	0.0829	0.0661
7	2254.8	2241.5	2247.5	0.0877	0.1125	0.0627
8	3022.4	2963.5	2960.8	0.1716	0.3055	0.0695

Some conclusions about the effect of the bolt position type can be seen from the results above.

- For the same torque, the eigenfrequencies for each mode get bigger in the order of Type A, B and C. For the type D, eigenfrequencies become smaller than the

previous Types. In the order of Type A, B, C and D, the number of the bolts used in the joints get larger, the joint become stiffer and the deformation decrease. However the mass effect must be taken into consideration. As the number of the bolts increasing, the mass also become larger. For the first three types, the effect of pressure distribution plays more role than the mass effect. But for Type D, mass effect plays important role. So during simulations, Young's modulus related to bolts position type and mass of the bolts are both need to be considered. The bolt mass is modeled with the elements around the bolt holes (figure 5.10), the density of these elements is set to be higher than the other part of the stucuture. The density here is  $33500\text{kg}/\text{m}^3$  in comparison with  $7806\text{kg}/\text{m}^3$  for other parts.

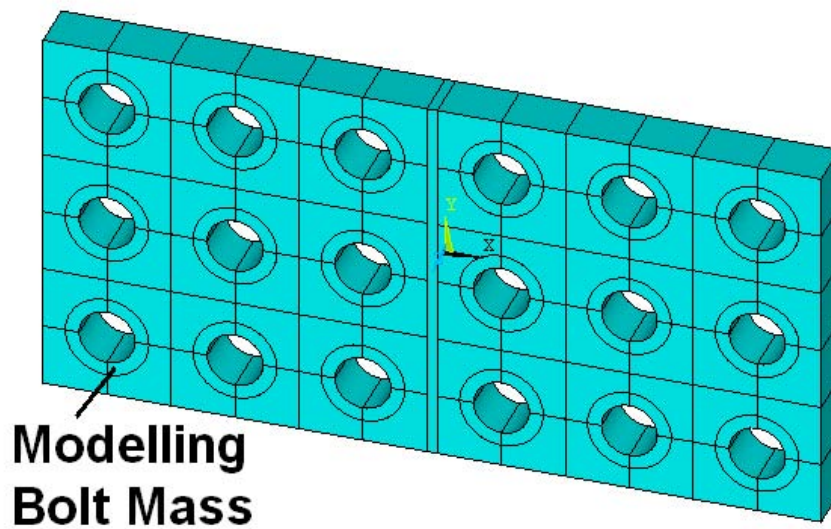


**Figure 5.10.:** Modeling the Bolt Mass

- For the same torque, damping ratio for some mode remain the same and some are tends to get smaller as the numbers of the bolts get larger. From type A to D, the joint become much stiffer since the normal force has become more equally contributed, the deformation becomes much less and the structures are assembled more tightly to each other. It is mentioned above that, the damping in the structure is depend on the deformation in the joint occurring due to a certain mode shape. It can be see from table 5.9 that, the damping almost the same at the bending mode with respect to y-axis (mode 1, 3, 4, 7) and it gets smaller at the torsion mode and mode that bending in z-axis direction (mode 3, 5, 6, 8) since

the defomation at the joint is small for the mode 1, 3, 4, 7 and the defomation at the joint is small big for mode 3, 5, 6, 8.

## 5.2. Simulation

The main purpose of this thesis is to investigate the relations between the joints characteristics and the modal parameters of the structure and to provide some basis, data bases and methods in order to improve the modeling of the joints so that the engineers can determine all the dynamic properties of the structure before the prototype created. Here simple simulation will be performed to introduce the method which is utilized in the simulation of the system with ANSYS. With the conclusions get from the experiment, the material parameters are modified to simulate the dynamic properties which will be compared with the experimental result.

### 5.2.1. Adjust Material Properties

Because there are difference between the experimental results and the simulated results, the material properties and the element properties of model must be updated (refine the mesh or using high order element) to get better estimation of eigenfrequencies. The joint damping will be discussed later. The density is selected as  $7806\text{kg}/\text{m}^3$  so that the simulated mass is close to the real mass. The mesh size and the element type

**Table 5.11.:** Experiment and Simulation Results with Different Element Type for Part A

	Experiment	Simulation solid45		Simulation solid95	
Mode	Freq(Hz)	Freq(Hz)	Diff(%)	Freq(Hz)	Diff(%)
1	1287.4	1318.6	2.4235	1311.8	1.8953
2	2459.1	2562.1	4.1885	2529.5	2.8628
3	3474.5	3519.7	1.3009	3504.0	0.8490
4	3549.3	3546.2	0.0873	3505.9	1.2228
5	4013.9	4167.6	3.8292	4104.4	2.2547
Average error(%)			2.36589		1.8169

need to be considered. The high order and low order element types are investigated. Here the result wiht the solid 45 element which is low order (8 nodes) element and the solid 95 which is high order (20 nodes) element is compared with the experimental result which showed in table 5.5. The comparison can be found in table 5.11.

The improvement is not significant, also the solid95 element consumes much time than solid45 elements.

Then the mesh need to be refined. The mesh size along the x direction of the part A is selected as  $2.29\text{mm}$  which lead to finer mesh. The density is  $7806\text{kg}/\text{m}^3$ , young's modulus  $E = 2.05E11\text{N}/\text{m}^2$ , the Poisson's ratio  $\nu = 0.33$ . The result of the simulation compared with the experimetal data is showed in table 5.12.

**Table 5.12.:** Experiment and Simulation Result with Finer Mesh for Part A

	Experiment	Simulation solid45		Simulation solid95	
Mode	Freq(Hz)	Freq(Hz)	Diff(%)	Freq(Hz)	Diff(%)
1	1287.4	1295.6	0.6369	1292.0	0.3573
2	2459.1	2497.9	1.5778	2480.4	0.8662
3	3474.5	3467.5	0.2015	3453.1	0.6159
4	3549.3	3513.4	1.0115	3494.9	1.5327
5	4013.9	4056.5	1.0613	4030.5	0.4136
Average error(%)			0.8978		0.75713

It can be seen from the result that, the simulated mass is  $m_s = 2.0789\text{kg}$  (solid45), real mass is  $m_r = 2.0790\text{kg}$ , error for simulated mass is  $0.00481\%$ . The result of eigenfrequencies is improved a lot for both element type. however, the solid95 consumes much time and the improvement is not significant. So it's better to perform simulation with solid45 element. When the mesh is refined, the proper density, Young's modulus and Possion ratio are defined, the eigenfrequency results with solid 45 element becomes close to the experiment results. The calculation time is also smaller than using solid95. So for the following simulations, the solid with finer mesh and solid45 element is chosen.

The update model parameters are checked with simulation for Part B and Part C. The simulated results can be found in table 5.13.

The error for simulated mass of Part B and Part C are  $0.2312\%$  and  $1.3601\%$  respectively. The simulation for eigenfrequencies of Part B and Part C shows pretty good results. So the material parameters will be set as density  $7806\text{kg}/\text{m}^3$ , young's modulus  $2.05E11\text{N}/\text{m}^2$  and possion's ratio  $0.33$  along with the refined mesh with soild 45 low order elements.

**Table 5.13.:** Experiment and Simulation Result with Finer Mesh for Part B and Part C

Mode	Part B			Part C		
	Experiment	Simulation solid45	Erro(%)	Experiment	Simulation solid45	Erro(%)
1	1244.9	1252.6	0.6147	3017.5	3063.1	1.4887
2	2669.8	2716.8	1.73	3701.7	3685.6	0.4368
3	3214	3213.4	0.0187			
4	3462.6	3427.3	1.03			
Average error(%)			0.8483			0.9628

### 5.2.2. Thin Layer Method

For the modeling of the joints, the thin layer method is applied. The detail of the method is introduced in the section 2.3. The finite elements model of the joint is showed in the figure 5.11. For the finite element modeling with thin layer, a thin layer will be embeded at the joint and the material properties are defined in the term of stress-strain matrix which also called tangent module for material showed in the equation ( 5.1 ). The element type of solid64 is utilized to satisfy this request. The thin layer has very small thickness. For ANSYS, the length-thickness ratio must be smaller than 16:1 for element type solid64.

$$\begin{bmatrix} \sigma_{xx} \\ \sigma_{yy} \\ \sigma_{zz} \\ \sigma_{xy} \\ \sigma_{yz} \\ \sigma_{zx} \end{bmatrix} = \begin{bmatrix} E_{11} & 0 & 0 & 0 & 0 & 0 \\ & E_{22} & 0 & 0 & 0 & 0 \\ & & E_{33} & 0 & 0 & 0 \\ & & & E_{44} & 0 & 0 \\ & & & & E_{55} & 0 \\ & & & & & E_{66} \end{bmatrix} \begin{bmatrix} \varepsilon_{xx} \\ \varepsilon_{yy} \\ \varepsilon_{zz} \\ \varepsilon_{xy} \\ \varepsilon_{yz} \\ \varepsilon_{zx} \end{bmatrix} \quad (5.1)$$

Since the interface has no stiffness in  $x$  and  $y$  directions, the terms  $E_{11}$  and  $E_{22}$  are disappeared.  $E_{33}$  represents the normal stiffness, whereas  $E_{55} = E_{66} = G$  defines the tangential stiffness of the joint. As the joint exhibits no stiffness for in-plane shearing,  $E_{44}$  is also zero. For numerical reasons all diagonal terms in equation ( 5.1 ) are not zero for ANSYS. So the values of  $E_{11}$ ,  $E_{22}$  and  $E_{33}$  are set to some small values in the calculation. These three parameters are set to 10, the  $E_{33}$  also will not affect the result too much and will chosen as  $E_{33} = 2E9N/m^2$ . For each bolt position type and each torque, it can be simulate with the different value of  $E_{55} = E_{66} = G$ .



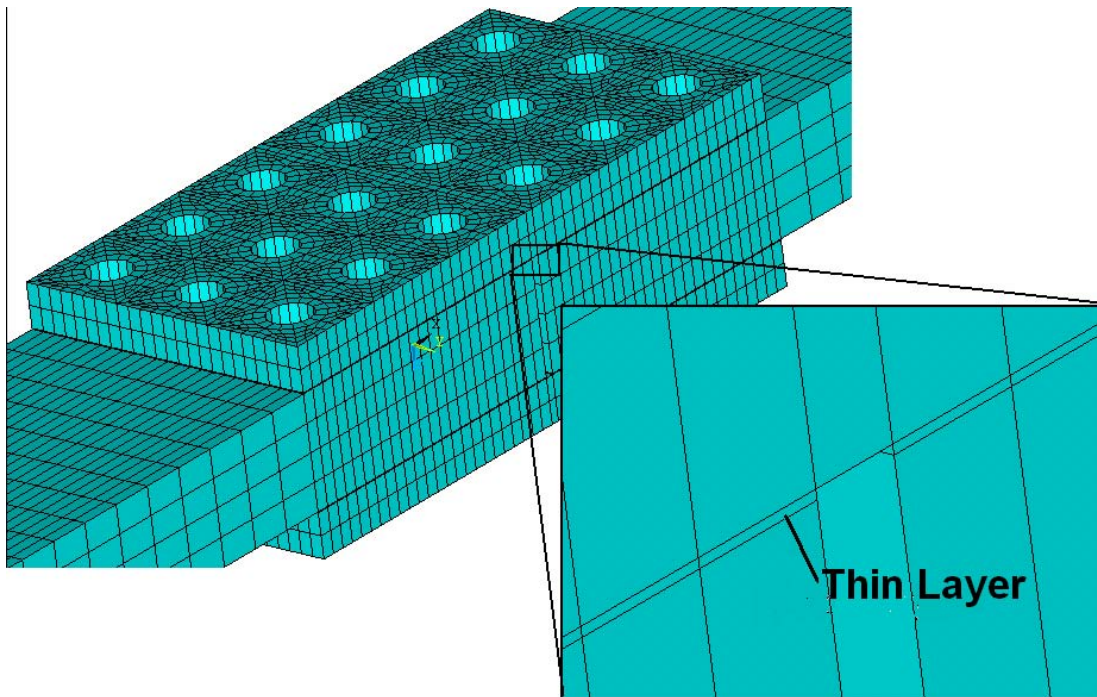


**Figure 5.11.:** FE Model for the Joint with Thin Layer Method

With the parameters provided, the structural dynamic analysis will be carried out. The modal analysis and harmonic analysis is performed. The modal analysis is used to obtain the eigenfrequencies and the harmonic analysis is used to simulate the damping properties.

### Eigenfrequency estimation with Modal Analysis

The modal analysis [4] [3] is used to calculate the eigenfrequencies. During this analysis, the structure is supposed to have a sandwich structure with thin layer in the middle glued together with each other. The damping will be ignored. Bolt position Type B and Type C with different torques with 20Nm and 30Nm are simulated. For this simulation, the module  $C$  will have the form of the equation ( 5.2 ) with the proper shear modulus  $G$  which gives the best result.

$$C = \begin{bmatrix} 10 & 0 & 0 & 0 & 0 & 0 \\ & 10 & 0 & 0 & 0 & 0 \\ & & 2e9 & 0 & 0 & 0 \\ & & & 10 & 0 & 0 \\ & & & & G & 0 \\ & & & & & G \end{bmatrix} \quad (5.2)$$

For Type B with torque  $20Nm$ , the shear modulus  $G = 3.5E8N/m^2$  shows good simulation results of eigenfrequencies which can be seen from table 5.14.

**Table 5.14.:** Experiment and Simulation Result for Type B with Torque 20Nm

Mode	1	2	3	4	5	6	7	8
Exp(Hz)	365.2	768.6	861.4	1636.5	1921.9	2212.2	2241.5	2963.5
Sim(Hz)	363.1	778	863.6	1637.8	1906.8	2210.7	2262.1	2978.8
Diff(%)	0.5784	1.2082	0.2547	0.0773	0.7902	0.0679	0.9092	0.5125

For Type B with torque  $30Nm$ , the shear modulus  $G = 4E8N/m^2$  shows good simulation results of eigenfrequencies which can be seen from table 5.15.

**Table 5.15.:** Experiment and Simulation Result for Type B with Torque 30Nm

Mode	1	2	3	4	5	6	7	8
Exp(Hz)	367.8	772.6	863	1643	1933.2	2215.3	2248.6	2966.2
Sim(Hz)	364.5	783.4	864.4	1642.2	1914.5	2214.4	2265.4	2982.1
Diff(%)	1.2944	0.6984	0.0656	0.3155	1.3845	0.2081	0.5968	0.4241

For Type C with torque  $20Nm$ , the shear modulus  $G = 9E8N/m^2$  shows good simulation results of eigenfrequencies which can be seen from table 5.16.

**Table 5.16.:** Experiment and Simulation Result for Type C with Torque 20Nm

Mode	1	2	3	4	5	6	7	8
Exp(Hz)	368.6	812.3	862.1	1646.1	1965	2229.1	2247.5	2960.8
Sim(Hz)	371.1	808.7	867.3	1662.5	1948.7	2227.7	2279.6	2972
Diff(%)	0.6737	0.4452	0.5996	0.9845	0.8365	0.0643	1.4081	0.3757

For Type C with torque  $30Nm$ , the shear modulus  $G = 10E8N/m^2$  shows good simulation results of eigenfrequencies which can be seen from table 5.17.

The result is summarized in the table 5.18 to see the interrelation between different bolt position type and different torque. It can be easily seen from table 5.18 that, the experiment results of eigenfrequencies and the simulation of eigenfrequencies are quite match each other, in other word, the eigenfrequency and mode shape can be simulated with very high accuracy.

**Table 5.17.:** Experiment and Simulation Result for Type C with Torque 30Nm

Mode	1	2	3	4	5	6	7	8
Exp(Hz)	370.5	818.7	863.5	1652.2	1975.4	2233.3	2252.5	2966.2
Sim(Hz)	371.7	811.7	867.7	1663.6	1952	2229.6	2282.2	2974.3
Diff(%)	0.3228	0.8665	0.4802	0.6833	1.1988	0.1674	1.2999	0.2735

**Table 5.18.:** Shear Modulus and Average Error for Type B, Type C with torque 20Nm, 30Nm

	Type B		Type C	
Torque (Nm)	20	30	20	30
G (N/m <sup>2</sup> )	3.50E+08	4.00E+08	9.00E+08	1.00E+09

The shear modulus is larger than Type B, this means Type C is stiffer. Since Type C put the bolts at edges of the structure which can reduce the deformation of the joints.

### Harmonic Analysis for Damping

For ANSYS, there is no complex modal analysis which can calculate the damping ratio directly. So the harmonic analysis is used to get FRF, then the damping can be obtained from the FRF using X-Modal II.

It is necessary for harmonic analysis to put constraint on the model. So the modal analysis is used to find three points constrain which will fix the system with less difference of eigenfrequencies of previous free-free boundary condition system.

The three point with the coordinates (0.180, 0, 0), (0.180, 0, 0.02015), (0.180, 0.0029, 0.01015) are chosen the comparison of the eigenfrequencies with and without constrain is showed in figure 5.19.

**Table 5.19.:** Eigenfrequencies for Type C and 30Nm With and Without Constrain

With (Hz)	371.7	811.7	867.7	1663.6	1952	2229.6	2282.2	2973.3
Without(Hz)	371.7	811.7	867.7	1663.6	1952	2229.6	2282.2	2974.3

The harmonic analysis is performed for the system with the joint damping which input into ANSYS model with the commend MP, DMPR. This commend is only available for harmonic analysis and can be used to modeling the hysteresis damping. The

damping ratio is given as 0.057 which is given in the reference [9]. The constraints with the three points given, the harmonic analysis with the frequency range from 200Hz to 3200Hz is carried out with the substep 300 which means the frequency resolution of 20Hz and 10Hz. Input force is at the node 4 of the structure and the output of the node 4 is recorded for the harmonic analysis. After the analysis, the result will be overlaid together with the experimental data get from the section 5.1.3. The plot can be found in figure 5.12.

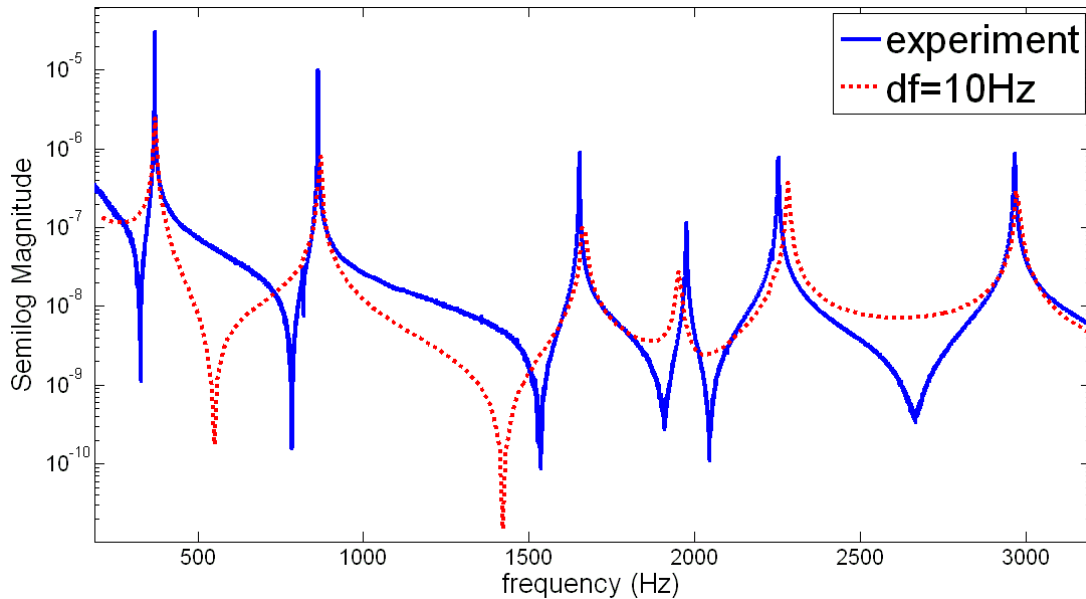


**Figure 5.12.:** Comparison of FRFs for simulation with 20Hz and experiment

For the simulation with ANSYS, the FRF obtained is displacement divided by the force, however the FRF obtained for the experiment is acceleration divided by the force. So the displacement signal needs to be transferred into acceleration signal in frequency domain in order to plot the FRFs in the same figure and compare them. The simulation FRF also needs to be transferred into the universal file formats for the further processing with X-Modal II. The relation between displacement signal and acceleration signal in the frequency domain can be seen in the equation (5.3).

$$\ddot{X}(f) = -(2\pi f)^2 X(f) = -\omega^2 X(f) \quad (5.3)$$

where  $\ddot{X}(f)$  is acceleration signal,  $X(f)$  is displacement signal,  $f$  is frequency,  $\omega$  is angular frequency [16].

It can be seen from figure 5.12 that the simulation overestimates the damping. So the same frequency resolution as the experimental data which is 0.25Hz must be

applied in order to compare the experimental results and simulated results. The comparison of the first two picks for the damping ratio given as 0.057 is showed in the figure 5.13 and the damping result for the first two pick will be summarized in the table 5.20.

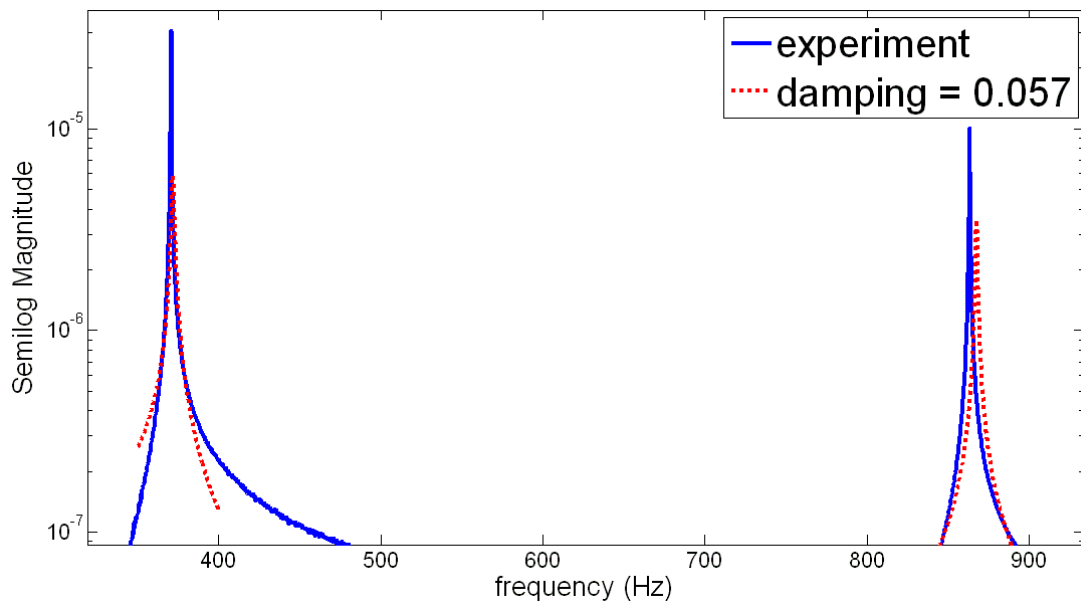


**Figure 5.13.:** Comparison of FRFs for simulation with 20Hz and experiment

The Simulation result with harmonic analysis is showed in the table 5.20. Actually the second mode is not appeared so well in this plot. So the mode we interested in is actually the first and third mode. The frequency range for the first mode is 350Hz to 400Hz and 840Hz to 890Hz for the third mode.

**Table 5.20.:** Comparison of Modal Parameters for First 2 Pick the Experiments and Simulation at 0.25Hz

	ANSYS		EXPERIMENT(4boltT 30N)	
	Frequency(Hz)	Damping(%)	Frequency(Hz)	Damping(%)
1st mode	371.8	0.2154	370.6	0.1147
3rd mode	867.7	0.0623	863.4	0.0594

It can be seen from the figure 5.13 and table 5.20 the damping is bigger than the experiment result and the curve also do not fit too well. Then the damping ratio must be adjusted using the simulation for the 1st modes. After several simulation, the

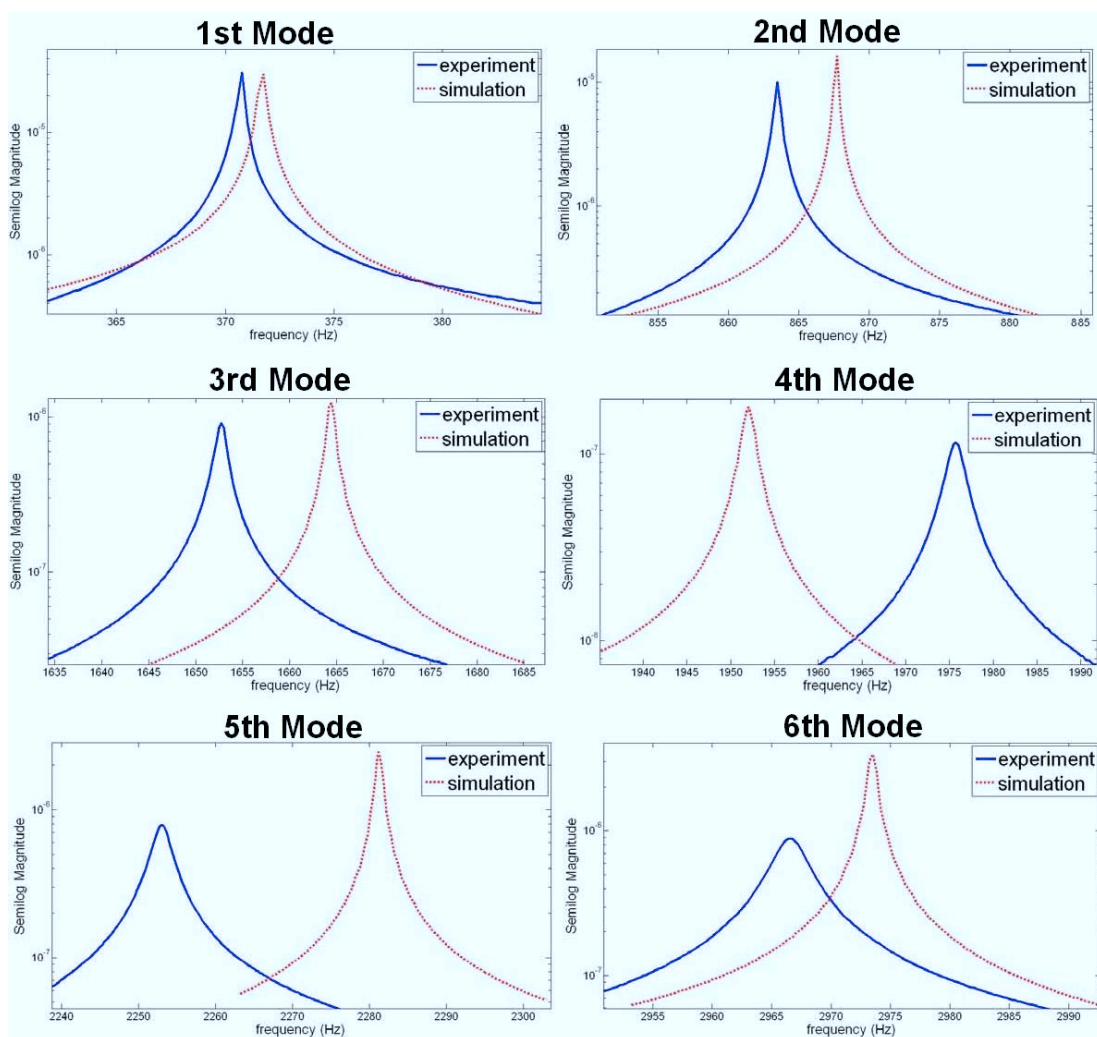


**Figure 5.14.:** Comparison of FRFs for simulation with 20Hz and experiment

**Table 5.21.:** Comparison of Modal Parameters for Experiments and Simulation at 0.25Hz

		ANSYS		Experiment		Error(%)	
mode	Frq(Hz)	frq (Hz)	Dmp(%)	frq (Hz)	Dmp(%)	freq	Damp
1st	360~ 385	371.7	0.0383	370.8	0.0328	0.2427	16.7683
2nd	850~ 890	867.7	0.011	863.5	0.0206	0.4864	46.6019
3rd	1645~ 1685	1664.2	0.0248	1652.9	0.0309	0.6836	19.7411
4th	1935~ 1975	1951.5	0.0386	1975.7	0.0529	1.2249	27.0321
5th	2263~ 2303	2280.5	0.0189	2253.1	0.0472	1.2161	59.9576
6th	2953~ 2993	2972.4	0.0121	2966.6	0.0469	0.1955	74.2004

damping ratio is updated to 0.01 which give the best curve fit to the experiment result. The simulation result is showed in figure 5.14 and table 5.21.

It can be seen from the figure 5.14 and table 5.21 that, the estimation of damping is not so good. the highest error for damping is 74%. The simulation showses good estimation for the first three mode and get worse for the mode in high frequency range. the result can be improved with using the material damping also with the constant frequency independent stiffness matrix coefficient  $\beta_j^\xi$ .





# 6. Conclusions and Recommendations

In this thesis, the structures with multiple joint characteristics are designed, constructed and investigated. The structures which satisfies the criteria is manufactured and used in the investigation of the system with multiple joint characteristics. Analytical approach is performed in order to select the modal parameter estimation methods. The experimental approach summarizes the influence caused by the different bolts position and the different torque, the influence is discussed with respect to not only the eigenfrequencies but also damping ratio. the simulation is performed to compare the simulated results with experimental results. In this Chapter several conclusions are made and some recommendations for further work are given.

## 6.1. Conclusions

- The PTD method showed best results for the analytical data with low damping, the PTD method is utilized to the analysis with the experimental data. The PTD method is high order time domain method. As time domain methods tend to provide the best results when a large frequency ranges and high order methods require more spatial data because they use only a limited subset of spatial data. For our structure the frequency range will be  $0-3000\text{Hz}$  and also the system use only 2 accelerometers which means there are few physical DOFs.
- For the same bolt position (identical pressure distribution), the eigenfrequencies for each mode will get bigger as the torque getting bigger. As the normal force at the joint getting bigger, the deformation at the joint gets smaller, the system gets stiffer which means young's modulus for the joint model get bigger.
- For the same bolt position (identical pressure distribution), modal damping ratios tend to get smaller as the torque getting bigger, since the damping in the structure is also dependent on the deformation in the joint occurring due to a certain mode shape. Damping ratios also get smaller as the torque get smaller.

Type A performs non-linearity which implies that, there must be enough bolts to make the structure perform linear.

- For the same torque, according to the order of the type A, B and C, the eigenfrequencies for each mode get bigger. But for the type D the eigenfrequency has become smaller than the previous bolt position type. In the order of type A, B, C, D, the number of the bolts used in the joints will get larger, the joint will become more and stiffer and the deformation will decrease. At the same time, the mass effect for the simulation must also take place. If the structure can be designed more heavier, this effect will be avoided.
- For the same torque, the damping ratio for the most modes also tends get smaller according to the order of the type A, B, C and D, which means that the numbers of the bolts get larger and the pressure get more well-distributed. From type A to D, the joint become much stiffer; the normal force has become more equally distributed; and the deformation becomes much less.
- The eigenfrequencies and the mode shapes can be calculated with finite elements method high accuracy. In this thesis, thin layer elements method is utilized and this method can simulate not only the different type of bolt position, but also the different torque used to fastening the bolts (pressure distribution).
- The damping ratio can also be simulated with finite element method. However, the result still shows big errors since the damping is very sensitive.

## 6.2. Recommendations

- For the structure used in the experiments, we only performed with part B and part C. In the further work the part A must also be utilized to perform more complicated structures with different joint characteristics. The structure is better to be more heavier, in order to avoid the massloading effect.
- More complex structure can be constructed with the Part A, Part B and Part C to investigate the system with joint characteristics.
- For the analytical approach, the noise must be take consider with respect to power, amplitude and so on. Also the model must be generated both in the time domain and frequency domain in order to check the effect of data sets with different domain to the MPE methods.

- 
- For the experiment, the shaker can be used instead of the impact hammer in further work, by the reason that the impact hammer cannot provide the structure with constant impulse. The shaker can solve this problem easily. But for this method, the massloading effect of the accelerometers will be need to take in consider.
  - For the experiment, instead of use the FRF signal of the system, the impulse signal can be directly used in order to investigate the MPE methods with the experimental data sets in time domain.
  - For the simulation, the stiffness and damping property are considered as constant in the thin layer at the joint. But in further work, the material and dynamic properties of system must be determined differently from position to position in the thin layer elements according to the bolt position. This must be providing much better result.
  - For simulation, ANSYS is used to perform the simulation, where the length to thickness ratio of the thin layer for solid 64 is smaller than 16:1. So other element type or other software such as Nastran which allows bigger length to thickness ratio must be applied for simulation.
  - As a consequence, investigattion of the effect of the thickness ratio of the thin layer and the elements nearby is required.
  - For the simulation, modeling the bolts with different methods will be also one of the interesting research fields for the further work, which can be referenced from referece [13]
  - For damping, more investigations are required.



# A. Appendix

## A.1. MATLAB codes

```
% Important MATLAB Command lines for Analytical Models

% signal parameters
df = 0.25; % Frequency Resolution
tt = 1/df; % Total Time
L = tt*2048; % Sampling Frequency Number
t = linspace(0,tt,L); % Array of Time
dt = t(3) - t(2); % Time Resolution
Lf = L/2;
f = linspace(0,df*(Lf-1),Lf); % Array of Frequency

% 2N system
A=[Z,M;M,C];
B=[-M,Z;Z,K];
[x,d]=eig(-inv(A)*B);
orig_lambda=diag(d);
[Y,I]=sort(imag(orig_lambda));
lambda=orig_lambda(I); % eigenfrequency

xx=x(:,I);
ma=xx.'*A*xx; % modal A
mb=xx.'*B*xx; % modal B

R(:, :, i)=psi(1:N,i)*psi(1:N,i)'./ma(i,i); %residue

%IRF
xt = 0;
```

```

for i = 1:2*N
    xt = xt +residu(i)./2*exp(lambda(i).*t);
end
%FRF
om=f.*2.*pi;
H = 0;
for i = 1:2*N
    H = H + residu(i)./(j.*om-lambda(i));
end

% Read Uff file
[UffDataSets , Info , errmsg] = readuff('xx.unv');

% Chage the UffDataSets
UffDataSets{3}.x = ;
UffDataSets{3}.measData = ;

%Write Uff file
Info = writeuff('xx.unv', UffDataSets);

```

## A.2. ANSYS codes

```

% Important ANSYS Command lines for Models
fini
/clear
/prep7

! Inputs
x_length=      ! length of the block
y_width=       ! (all units in m)
z_thick=
exs=           ! Young's modulus pipe wall
nuxs=          ! Poisson number pipe wall
denss=         ! pipe density
DMPR_ratio_1 =

```

```
! Divisions
t1l=25          ! Divisions over width
tlw=24          ! Divisions over height
t1t=4           ! Divisions over thickness

! Define material properties
ET,1,SOLID45
MAT,1
MP,EX,1,exs
MP,NUXY,1,nuxs
MP,DENS,1,denss
ALPHAD, DMPR_ratio_1

! Creat the block
block,0,x_length,0,y_width,0,z_thick

! Discretize
lsel,s,length,,x_length
lesize,all,,,t1l
lsel,s,length,,y_width
lesize,all,,,tlw
lsel,s,length,,z_thick
lesize,all,,,t1t

! Mesh
type,1
MAT,1
vmesh,all
allsel
sftran

! Save this model
/solu
CDWRITE,comb,E:\xx\xx

! Read model
CDREAD,comb,E:\xx\xx
```

```
! Move or Copy the volume
vgen ,(number) ,all , , ,x,y,z , , ,1(0)

! Modal Analysis
/SOLU
ANTYPE,2
MODOPT,damp,25 ,5 ,4000
MXPAND,25
allsel
solve
finish

! Harmonic Analysis
/SOLU
ANTYPE,3          ! Harmonic response analysis
HROPT,FULL        ! Full harmonic response
HROUT,on          ! Results as amplitudes & phase angles
NSUBST,160        ! Intervals within freq. range
HARFRQ,1,2        ! Frequency range 1 to 2
KBC,1             ! Step boundary condition

!constrain
nselect ,s ,loc ,x,0.180
nselect ,r ,loc ,y,0.0
nselect ,r ,loc ,z,0.0
D,ALL,ALL

FK,462 ,FZ,-1      ! Force

! Output file control
outres ,all ,none
outres ,NSOL,ALL,neednode
ALLSEL
SOLVE
FINISH
```



### A.3. Blueprint

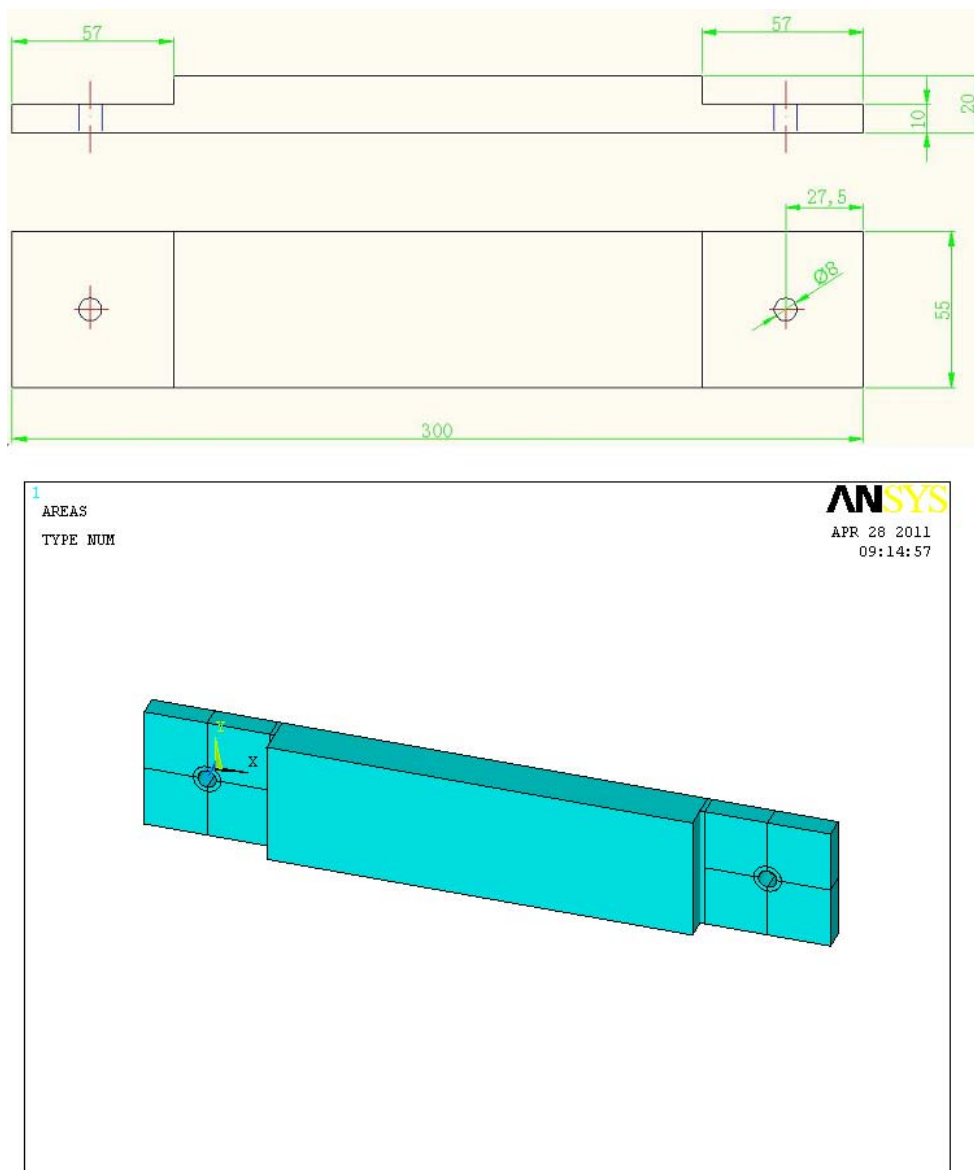


**Figure A.1.:** Drawing of the structure A

For the further work, structure A must be utilized. and it can constructed to the structure showed in figure A.4.

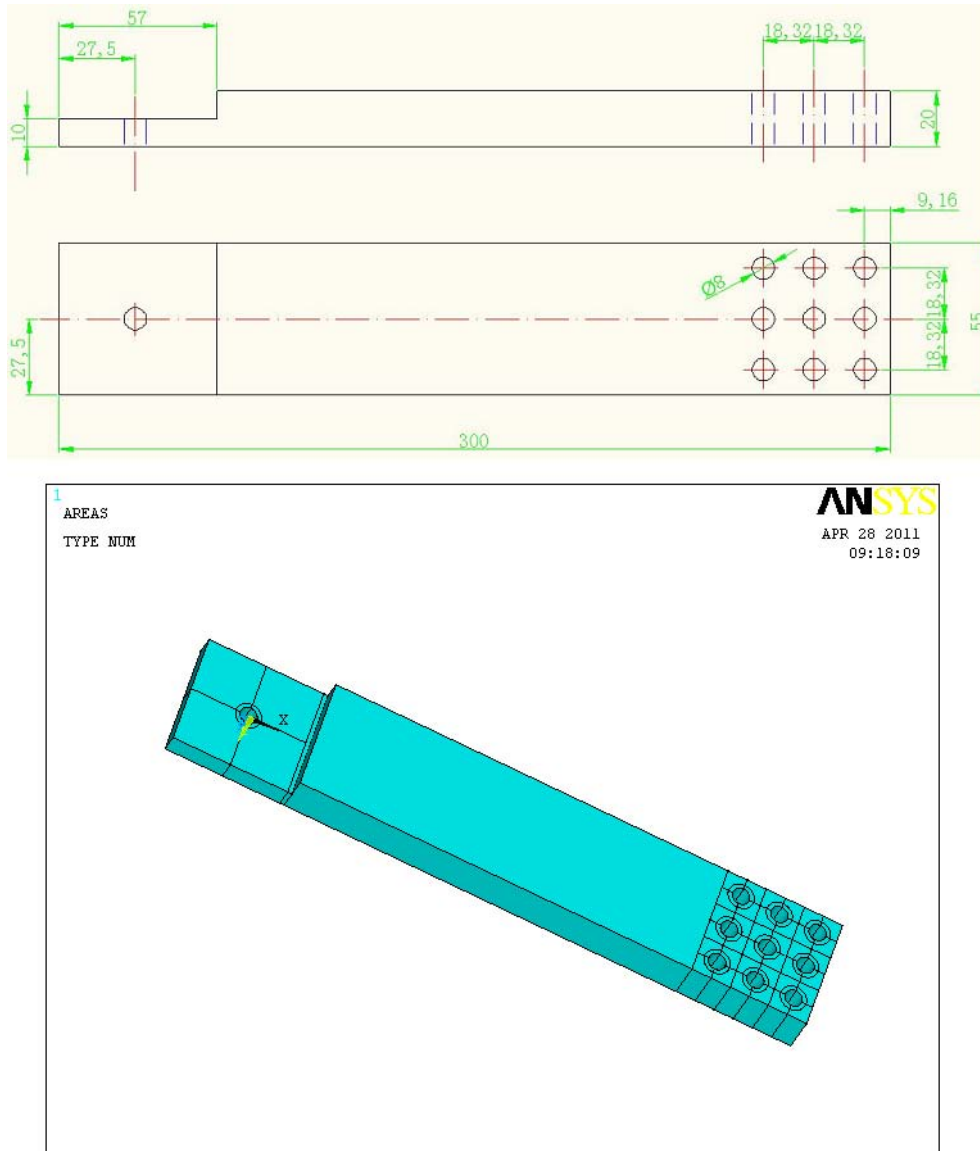


Figure A.2.: Drawing of the structure B

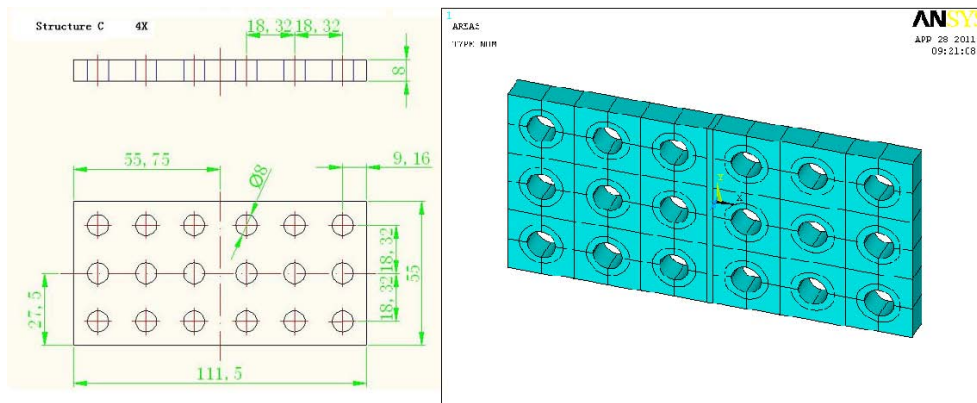


Figure A.3.: Drawing of the structure C

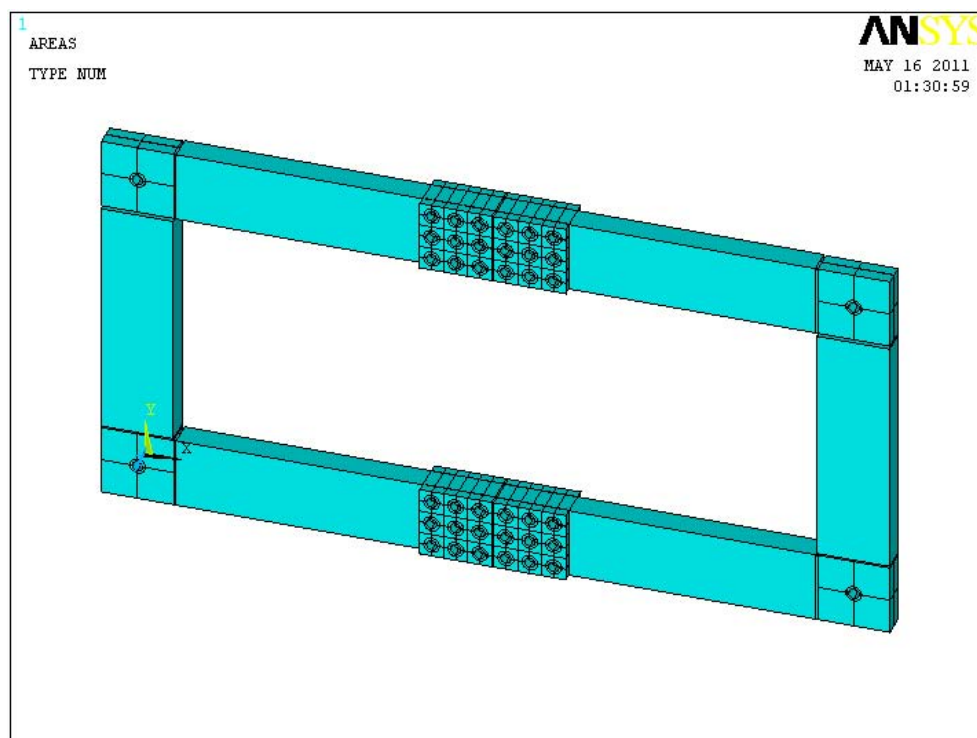


Figure A.4.: Drawing of the total structure



# List of Figures

1.1. Examples of mechanical systems for daily life with numerous joints . . . . .	1
2.1. Dynamic models interrelation . . . . .	6
2.2. Model with N degrees of freedom . . . . .	7
2.3. Laplace plane pole location[19] . . . . .	8
2.4. Classification of modal analysis methods[15] . . . . .	13
2.5. Schematic diagram of a joint with a thin layer element . . . . .	21
3.1. Drawing of the assembled structure . . . . .	25
3.2. Meshing the structure A . . . . .	25
3.3. Eigenfrequencies of the Structure with different Meshing density . . . . .	26
3.4. Eigenfrequencies of the assembled Structure . . . . .	28
4.1. Signals of SISO modal model data sets . . . . .	32
4.2. MPE user interface of X modal II [17] . . . . .	35
4.3. Consistency Diagram for Experiment Datasets . . . . .	36
4.4. Pole Surface Density Diagram for Experiment Datasets . . . . .	36
4.5. Pole Selection Methods with X-Modal II . . . . .	37
5.1. Part A, Part B and Part C . . . . .	46
5.2. Experiment Setup . . . . .	46
5.3. Discretization of the Measured Structure . . . . .	47
5.4. Massloading Effect for Part A at 1st Mode . . . . .	48
5.5. Impact Hammer Experiment for Part C . . . . .	50
5.6. Nodes for the part A, part B and part C . . . . .	51
5.7. Types of Different Positions of Bolts . . . . .	51
5.8. Real System of Bolt Position Type D . . . . .	52
5.9. The Total System with Bolt Position Type A . . . . .	52
5.10. Modeling the Bolt Mass . . . . .	57
5.11. FE Model for the Joint with Thin Layer Method . . . . .	61
5.12. Comparison of FRFs for simulation with 20Hz and experiment . . . . .	64

5.13. Comparison of FRFs for simulation with 20Hz and experiment . . . .	65
5.14. Comparison of FRFs for simulation with 20Hz and experiment . . . .	66
A.1. Drawing of the structure A . . . . .	77
A.2. Drawing of the structure B . . . . .	78
A.3. Drawing of the structure C . . . . .	79
A.4. Drawing of the total structure . . . . .	79

# List of Tables

3.1. Comparison with different meshing density . . . . .	26
4.1. Properties of the SISO modal model data set . . . . .	32
4.2. The Values of Mass, Stiffness and Damping . . . . .	34
4.3. Properties of the MIMO spatial model data set . . . . .	34
4.4. The Exact Properties for SISO Modal Model . . . . .	38
4.5. The Average Error with SISO Modal Model at Frequency Resolution 1Hz . . . . .	38
4.6. The Average Error with SISO Modal Model at Frequency Resolution 0.5Hz . . . . .	38
4.7. The Average Error with SISO Modal Model at Frequency Resolution 0.25Hz . . . . .	39
4.8. The Average Error with SISO Modal for Different Frequency Resolutions	39
4.9. The Exact Properties for MIMO Modal Model . . . . .	40
4.10. The Average Error with MIMO Modal Model for Different Frequency Resolutions . . . . .	41
4.11. The Exact Properties for MIMO Spatial Model . . . . .	41
4.12. The Average Error with MIMO Spatial Model(1Hz and Method B) . .	42
4.13. The Average Error with MIMO Modal Model with Random Noise . .	42
4.14. The Average Error with MIMO Modal Model with Different Noise Amplitude . . . . .	43
5.1. Mass of Each Part of Real Structure . . . . .	47
5.2. Effect of Mass attached and cable for Input -6z Output 1z . . . . .	48
5.3. Effect of Mass attached and cable for Input -6z Output 3z . . . . .	49
5.4. The Experiments performed . . . . .	52
5.5. Modal Parameters for Part A, Part B and Part C . . . . .	53
5.6. Modal Parameters for Type A with Torque 10Nm, 20Nm and 30Nm .	54
5.7. Modal Parameters for Type B with Torque 20Nm and 30Nm . . . . .	54
5.8. Modal Parameters for Type C with Torque 20Nm and 30Nm . . . . .	55

5.9. Modal Parameters for Torque 30Nm with Type A,B,C,D . . . . .	56
5.10. Modal Parameters for Torque 20Nm with Type A,B,C . . . . .	56
5.11. Experiment and Simulation Results with Different Element Type for Part A . . . . .	58
5.12. Experiment and Simulation Result with Finer Mesh for Part A . . . .	59
5.13. Experiment and Simulation Result with Finer Mesh for Part B and Part C	60
5.14. Experiment and Simulation Result for Type B with Torque 20Nm . .	62
5.15. Experiment and Simulation Result for Type B with Torque 30Nm . .	62
5.16. Experiment and Simulation Result for Type C with Torque 20Nm . .	62
5.17. Experiment and Simulation Result for Type C with Torque 30Nm . .	63
5.18. Shear Modulus and Average Error for Type B, Type C with torque 20Nm, 30Nm . . . . .	63
5.19. Eigenfrequencies for Type C and 30Nm With and Without Constrains .	63
5.20. Comparison of Modal Parameters for First 2 Pick the Experiments and Simulation at 0.25Hz . . . . .	65
5.21. Comparison of Modal Parameters for Experiments and Simulation at 0.25Hz . . . . .	66



# Bibliography

- [1] Douglas E. Adams. Modal parameter estimation report. Technical report, University of Cincinnati Structural Dynamics Research Laboratory, 01 1998.
- [2] Cyril M. Harris Allan G. Piersol, Thomas L. Paez. *Harris' shock and vibration handbook*. ISBN 0071508198, 9780071508193. McGraw Hill Professional, 2009.
- [3] Inc. ANSYS. Ansys structural analysis guide ansys release 9.0. Technical report, ANSYS, Inc., 11 2004.
- [4] ANSYS, Inc. *ANSYS 11.0 Reference*, 2007.
- [5] D.L. Brown A.W.Phillips, R.J. Allemang. Autonomous modal parameter estimation: Methodology. Technical report, Structural Dynamics Research Laboratory, University of Cincinnati, Cincinnati, OH 45221-0072 USA.
- [6] Primoz Cermelj. *UFF File Reading and Writing*. MATLAB Center, <http://www.mathworks.com/matlabcentral/fileexchange/6395-uff-file-reading-and-writing>, 02 2011.
- [7] T. N. Hatzigogos D.A. Karampatakis. A model to describe creeping behavior of thin-layer element for interfaces and joints. Technical report, Laboratory of Soil Mechanics and Foundations, Aristotle University of Thessaloniki.
- [8] Jeffrey L. Dohner. On the development of methodologies for constructing predictive models of structures with joints and interfaces. Technical report, The Structural Dynamics Department, Sandia National Laboratories, 2000.
- [9] S. Bograd et al. Modeling the dynamics of mechanical joints. *Mechanical Systems and Signal Processing*, 2011.
- [10] Angel Moises Iglesias. Investigating various modal analysis extraction techniques to estimate damping ratio. Master's thesis, Virginia Polytechnic Institute and State University, 06 2000.

- [11] Sheldon Imaoka. Addendum to structural damping. Technical report, ANSYS.net Tips and Tricks, 04 2008.
- [12] LMS Inc. Lms polymax - a revolution in modal parameter estimation.
- [13] Beom-Soo Kang Jeong Kim, Joo-Cheol Yoon. Finite element analysis and modeling of structure with bolted joints. *Applied Mathematical Modelling*, 31:895–911, 2007.
- [14] LMS international. *Enhanced Exploitation of Vibration Test Data by the Polymax Modal Parameter Estimation Method*, Proceedings of the 5th International Symposium on Environmental Testing for Space Programmes. European Space Agency, 08 2004.
- [15] Maia and Silva et al. *Theoretical and Experimental Modal Analysis*. Research Studies Press LTD, Baldock, Herfordshire, England, 1998.
- [16] Colin Merce. Acceleration, velocity and displacement spectra-omega arithmetic-prosig signal processing tutorials. Technical report, Prosig Inc., 11 2006.
- [17] Allyn W. Phillips. Tutorial for modal parameter estimation. Technical report, University of Cincinnati, 12 2002.
- [18] A.W. Phillips R.J. Allemang, D.L. Brown. Survey of modal techniques applicable to autonomous/semi-autonomous parameter identification. *PROCEEDINGS OF ISMA2010*, pages 3331–3371, 2010.
- [19] R.J.Allemang. *Vibrations: Analytical and Experimental Modal Analysis*. 02 1999.
- [20] R.J.Allemang. *Vibrations: Experimental Modal Analysis*. Structural Dynamics Research Laboratory – Department of Mechanical, Industrial and Nuclear Engineering – University of Cincinnati, 03 1999.
- [21] D.L.Brown R.J.Allemang. A unified matrix polynomial approach to modal identification. *Journal of Sound and Vibration*, 211(3):301–322, 1998.
- [22] L.Gaul S.Bograd, A.Schmit. Joint damping prediction by thin layer elements. Technical report, Institute for Applied and Experimental Mechanics, Uni Stuttgart, Pfaffenwaldring 9, 70550 Stuttgart, Germany.
- [23] L.Gaul S.Bograd, A.Schmit. Modeling of damping in bolted structures. Technical report, Institute for Applied and Experimental Mechanics, Uni Stuttgart, 2007.

[24] UC-SDRC. *X modal II Reference*, 05 2011.

[25] UC-SDRL. *X-Modal tutorial*. University of Cincinnati, Structural Dynamics Research Laboratory.